Progress Report on Work Performed on the LIBRA Design During the Period 1 February 1987 to 31 January 1988

B. Badger, G. Moses, R. Engelstad, G. Kulcinski, E. Lovell, J. MacFarlane, Z. Musicki, R. Peterson, M. Sawan, I. Sviatoslavsky, L. Wittenberg

January 1988

UWFDM-754

FUSION TECHNOLOGY INSTITUTE

UNIVERSITY OF WISCONSIN

MADISON WISCONSIN

Progress Report on Work Performed on the LIBRA Design During the Period 1 February 1987 to 31 January 1988

B. Badger, G. Moses, R. Engelstad, G. Kulcinski,
E. Lovell, J. MacFarlane, Z. Musicki, R. Peterson,
M. Sawan, I. Sviatoslavsky, L. Wittenberg

Fusion Technology Institute
University of Wisconsin
1500 Engineering Drive
Madison, WI 53706

http://fti.neep.wisc.edu

January 1988

UWFDM-754

PROGRESS REPORT ON WORK PERFORMED ON THE LIBRA DESIGN DURING THE PERIOD 1 FEBRUARY 1987 TO 31 JANUARY 1988

B. Badger, G. Moses, R. Engelstad, G. Kulcinski,
E. Lovell, J. MacFarlane, Z. Musicki, R. Peterson,
M. Sawan, I. Sviatoslavsky, L. Wittenberg

Fusion Technology Institute
University of Wisconsin-Madison
1500 Johnson Drive
Madison, WI 53706-1687

January 1988

UWFDM-754

Agenda for LIBRA Review Meeting, 28–29 January 1988

Channel Formation	Peterson
30 MV Accelerator Design	Smith
Target Injection	Peterson
Cavity Clearing	Peterson/Moses
Neutronics	Moses
Cavity Design	Kulcinski
Tritium Retention	Kulcinski

Plasma Channels are Required for Repetitive Light Ion Fusion

Purpose of Channels: To carry beams of ions from ion diodes to a target efficiently and repetitively, to provide standoff for ion diode protection, and to allow time-of-flight beam bunching.

How They Work: A discharge electron current forms azimuthal magnetic fields that confine ions to the channel and rarifies the channel center to minimize collisional ion energy loss.

How a Channel is Formed: Two lasers preionize narrow tubes of the background gas that intersect at the target, then a high voltage capacitor is discharged across the ends of these tubes.

SCHEMATIC OF PLASMA CHANNEL

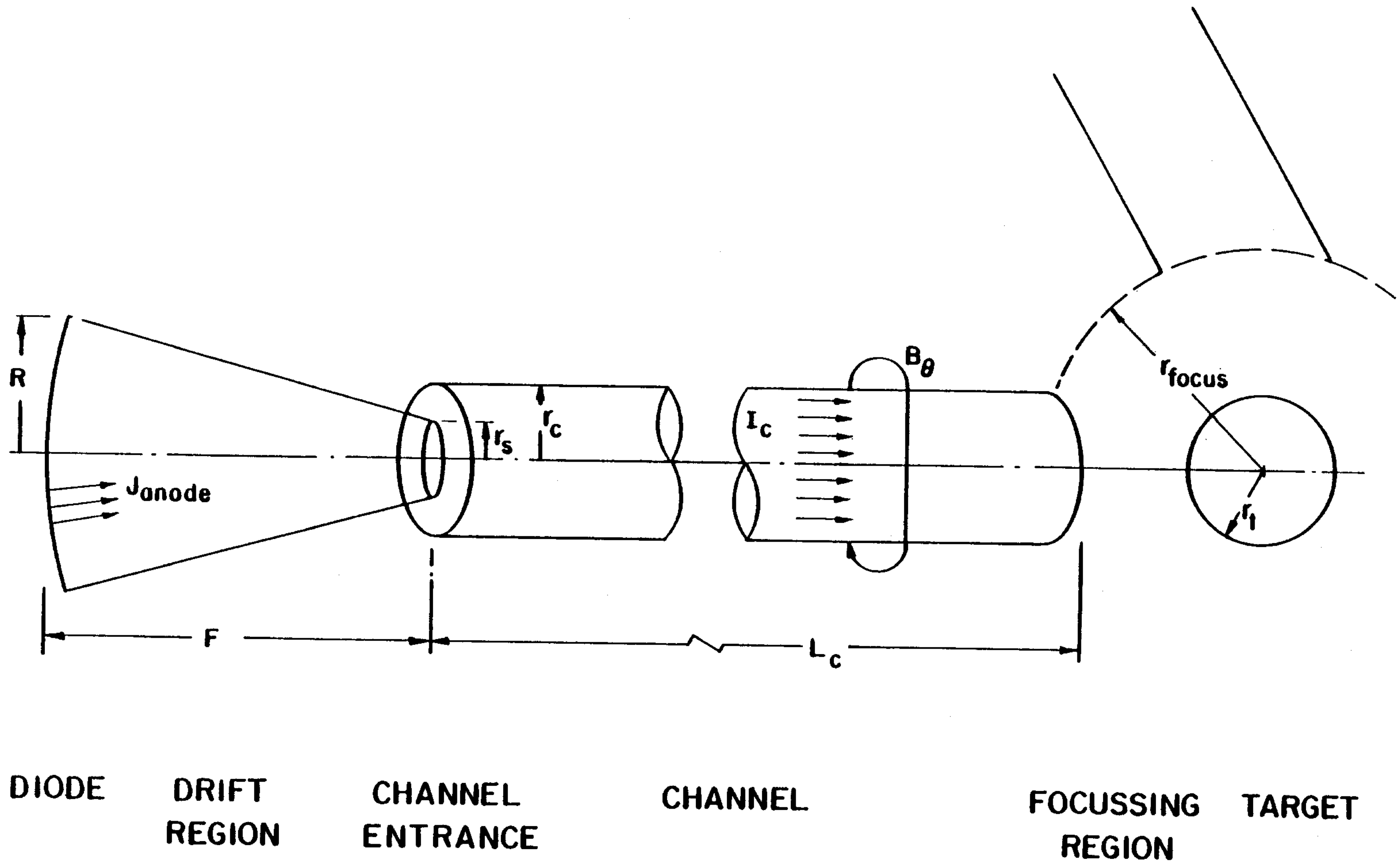

Channel Parameters for LIBRA

Channel Length	5.4 m
Channel Radius	0.5 cm
Target Chamber Gas	3.55×10^{17} cm^{-3} Ar + 0.2% Li
Average Beam Ion Energy	30 MeV
Maximum Injection Angle into Channel	0.15 radians
Ion Species	Li^{+3}
Ion Power Injected into Channel	9.5 TW
Bunching in Channel	4.4
Ion Power on Target per Channel	25 TW
Ion Energy Loss in Channel	25%
Fraction of Ions Reaching Target	80%
Number of Main Pulse Beams	16
Number of Prepulse Beams	2
Number of Channels	36
Maximum Discharge Current	100 kA
Discharge Current Shape	Double Pulse
Required Magnetic Field at Channel Radius	28 kG

Comparison Between LIBRA Channels and Channels in Other Facilities

	EAGLE	TDF	LIBRA
Length (m)	4.9	3	5.4
Radius (cm)	0.63	0.5	0.5
Ion Species	D	Li	Li
Ion Energy (MeV)	6.3	30	30
Injection Angle (rad)	0.09	0.15	0.15
Background Gas	He+1% Xe	N_2	Ar+0.2% Li
Gas Density (cm^{-3})	$2x10^{19}$	$1x10^{18}$	$3.55x10^{17}$
Max. Discharge Current (kA)	30	100	100
Ion Energy Loss (%)	10	25	25
Number of Channels	46	24	36

Computer Simulations of Plasma Channel Formation

ZPINCH Computer Code:
- 1-D (radial)
- Lagrangian hydrodynamics
- MHD
- Magnetic Field Diffusion
- Current Profile and History
- Radiation Diffusion
- Tabulated LTE equation-of-state

Optimization of Channel Parameters:
- Done for N_2 (TDF)
- Vary laser width
- Vary current history

Channel Formation Calculations for LIBRA:
- Done for Ar + 0.2% Li
- Done for best laser and current parameters in N_2 optimization
- Done with and without radiation transport

Double Pulse Channel Discharge Current Profile

First pulse initiates radial shock that reduces gas density in channel.

Second pulse creates azimuthal magnetic field, but can pinch channel.

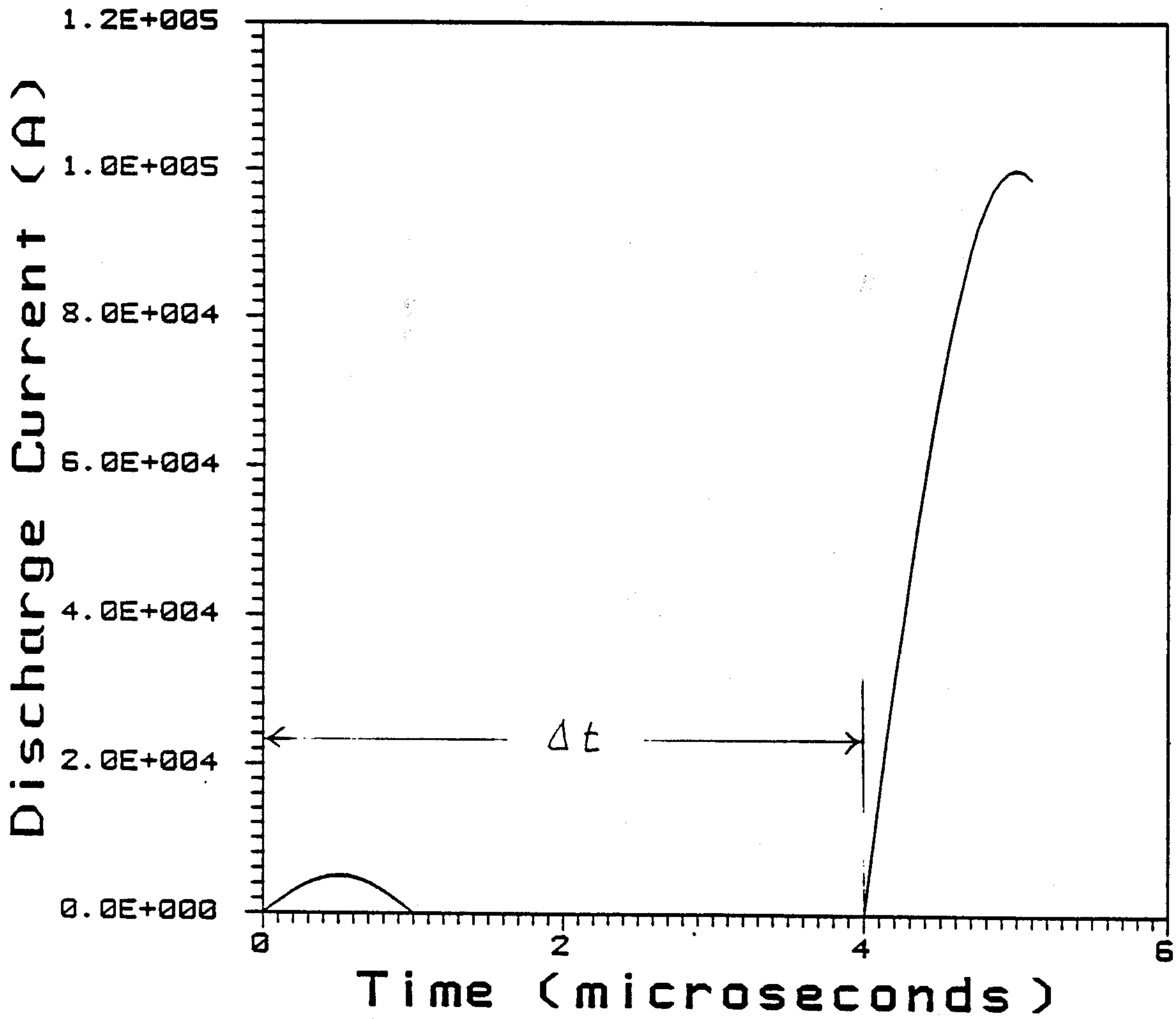

Time delay Δ*t* is an independent variable in ZPINCH input.

Laser Profile is Gaussian

Gaussian laser profile leads to a Gaussian initial gas temperature profile in the channel.

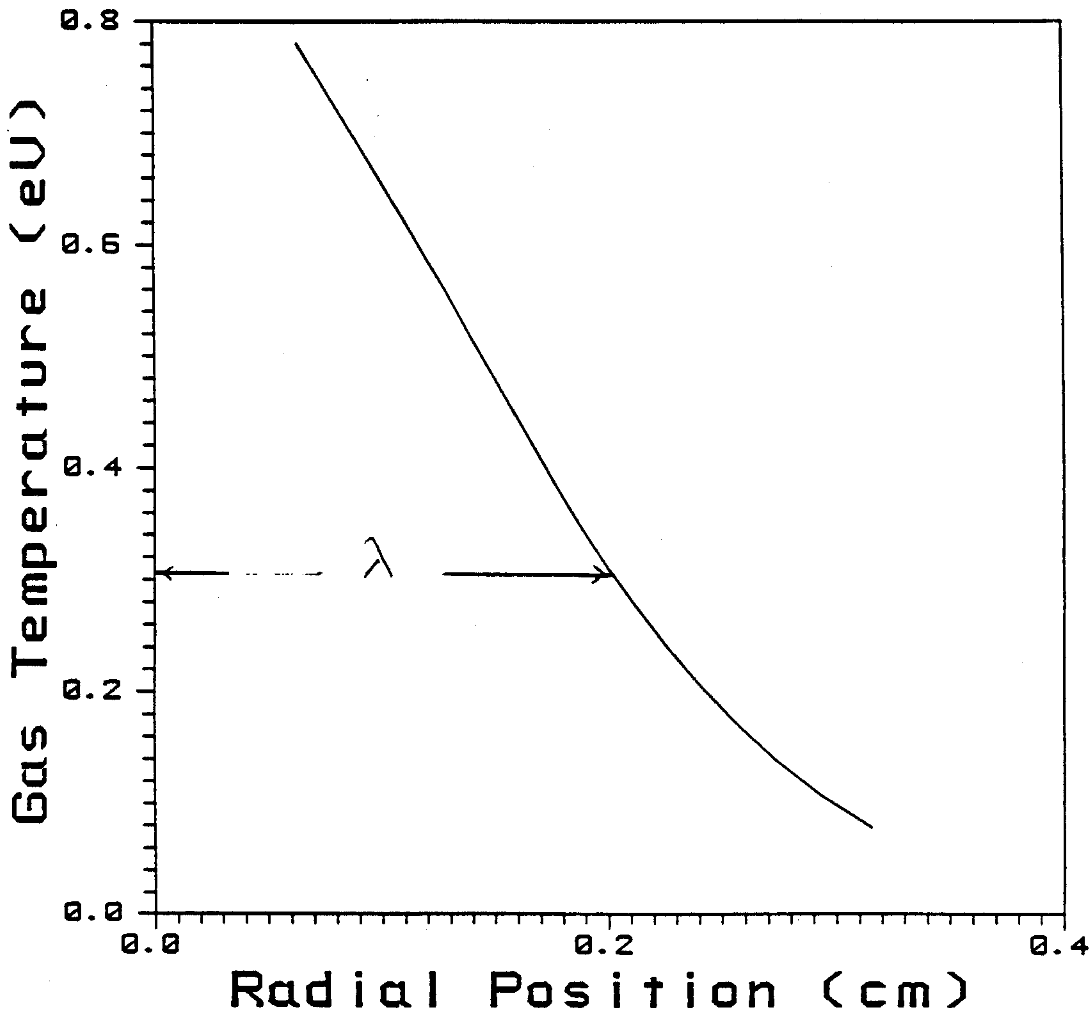

Gaussian width is an independent variable in ZPINCH input.

Matrix of Z-PINCH Calculations

Time Delay (μs)

Laser Radius (mm)	1	2	3	4	5
1	X	X			
2	X				
3	X	X			
4	X				
5	X	X	X	X	X

PARAMETRIC STUDY FOR N_2 CHANNELS

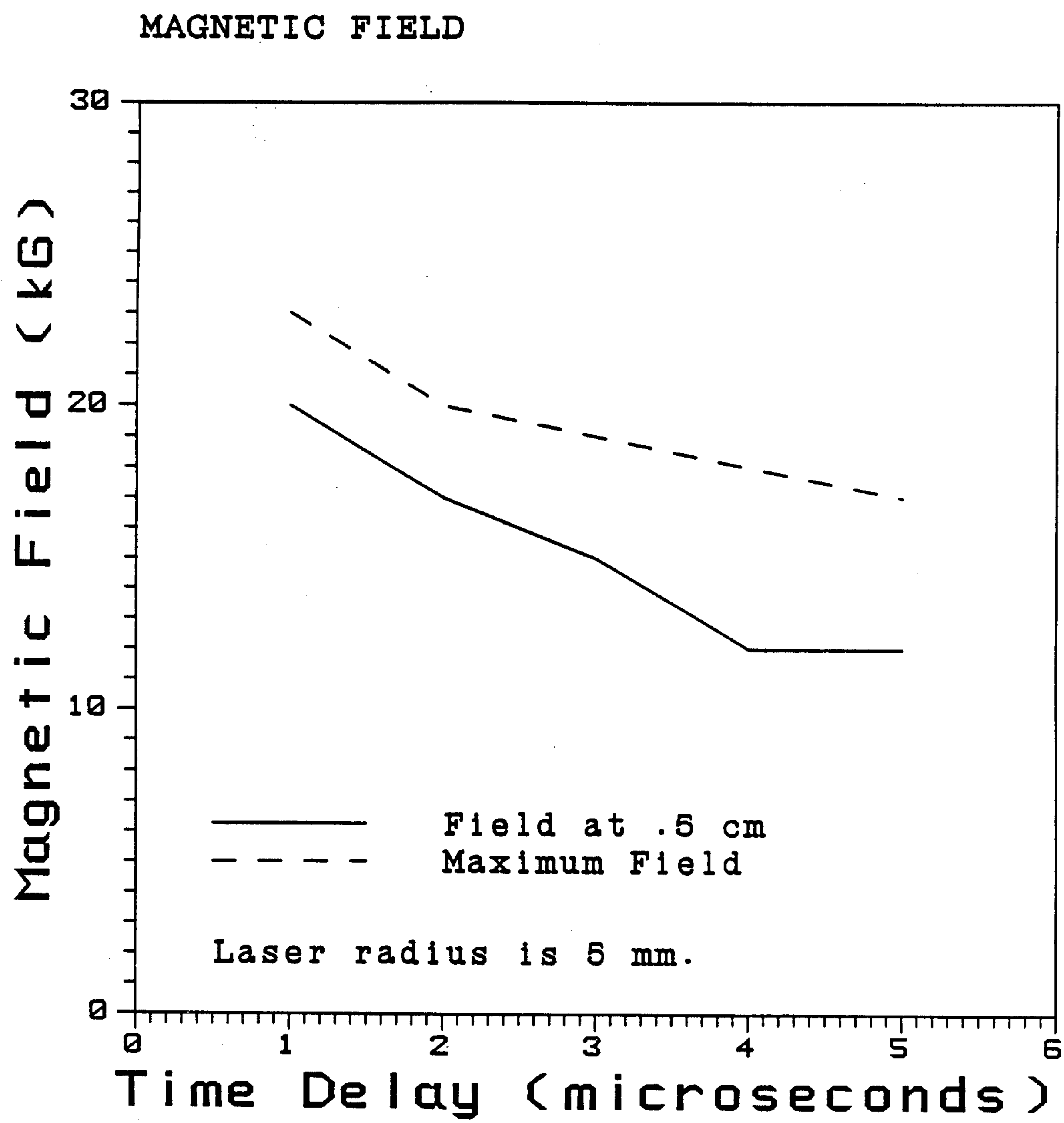

PARAMETRIC STUDY FOR N_2 CHANNELS

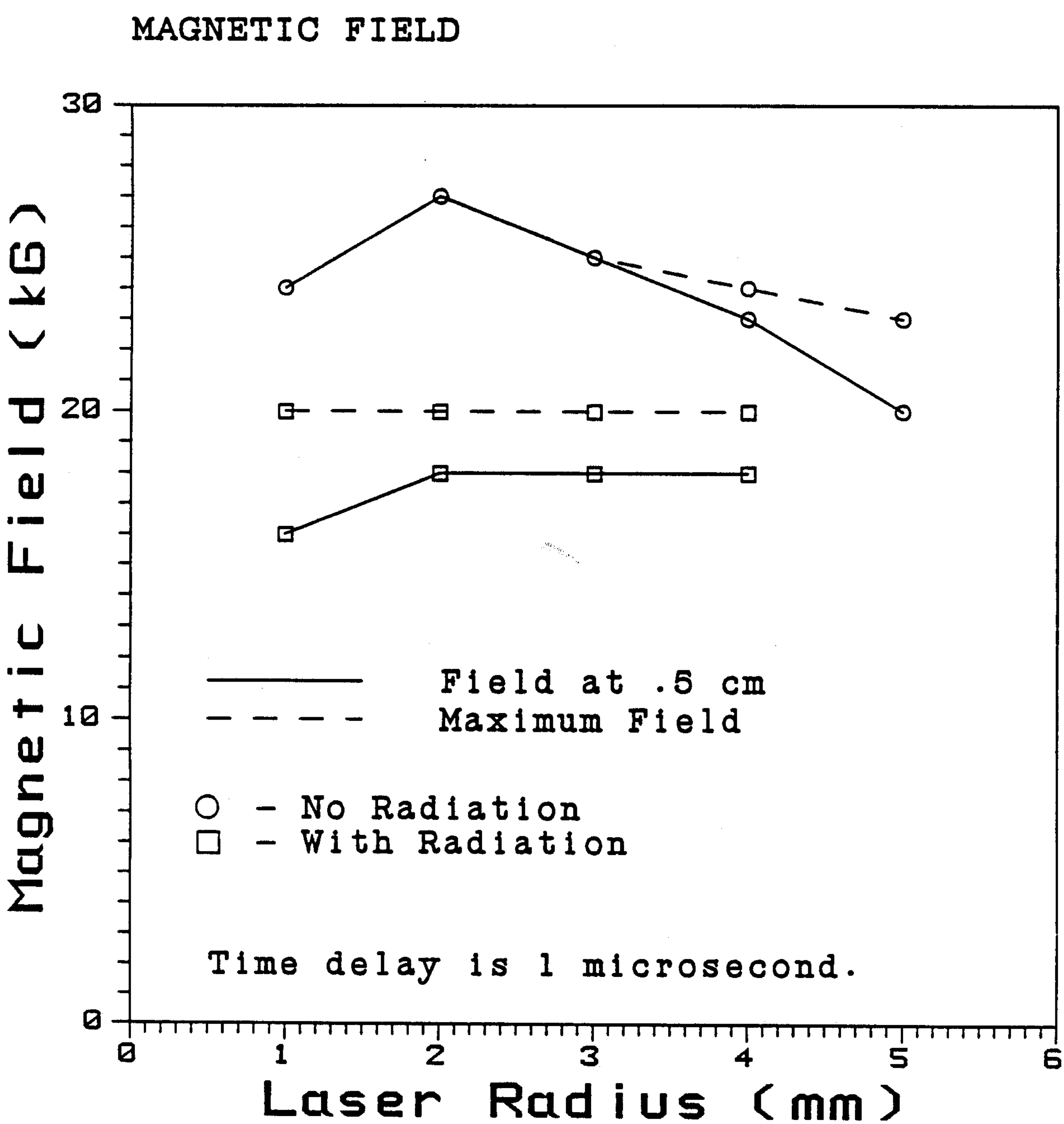

BEST FREE STANDING CHANNEL–NO RADIATION

$\Delta T = 1\ \mu s$, Laser Width = 2 mm
Gas = 10^{18} cm^{-3} N_2

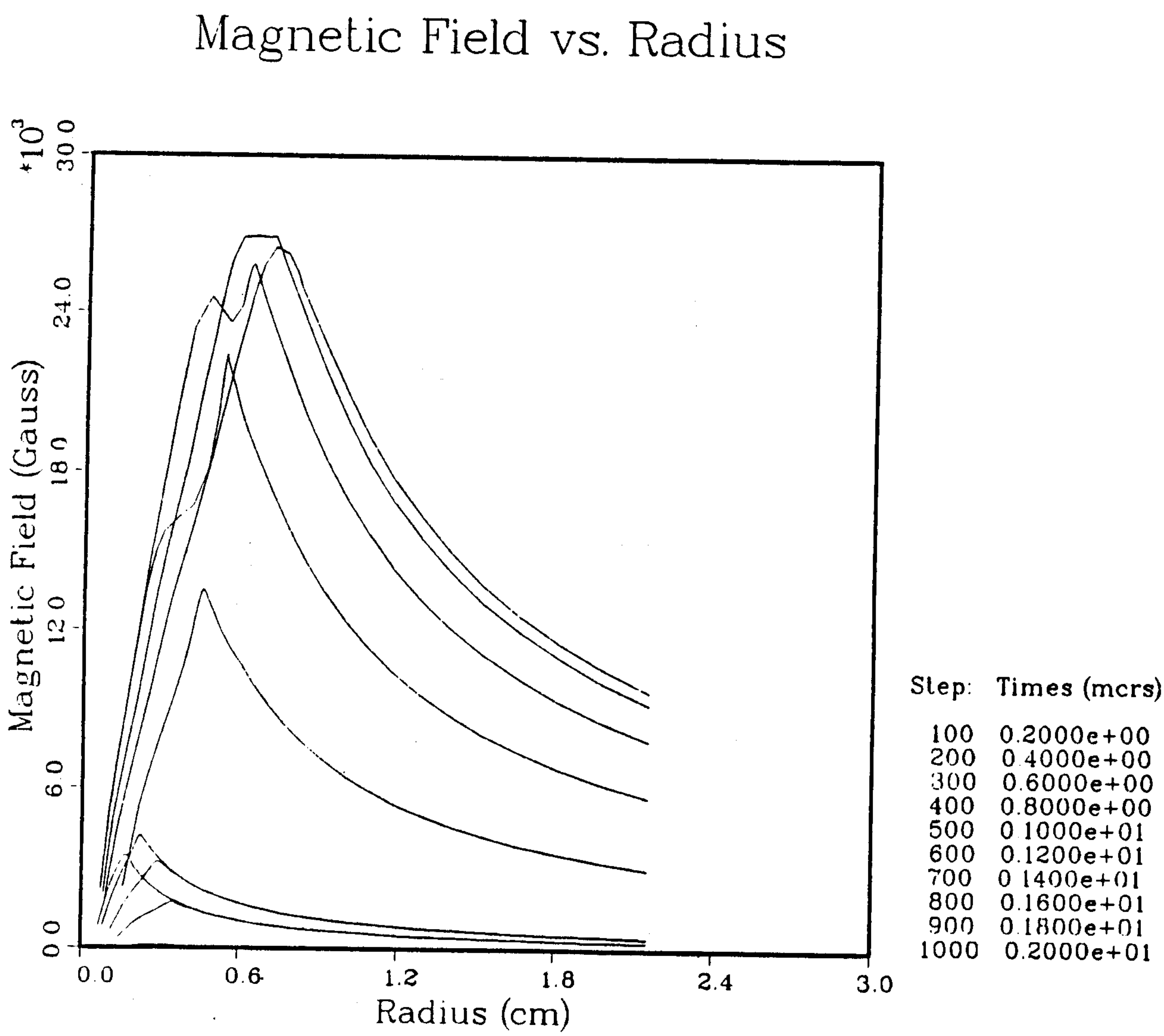

BEST FREE STANDING CHANNEL WITH RADIATION

$\Delta T = 1\ \mu s$, Laser Width = 2 mm
Gas = 10^{18} cm^{-3} N_2

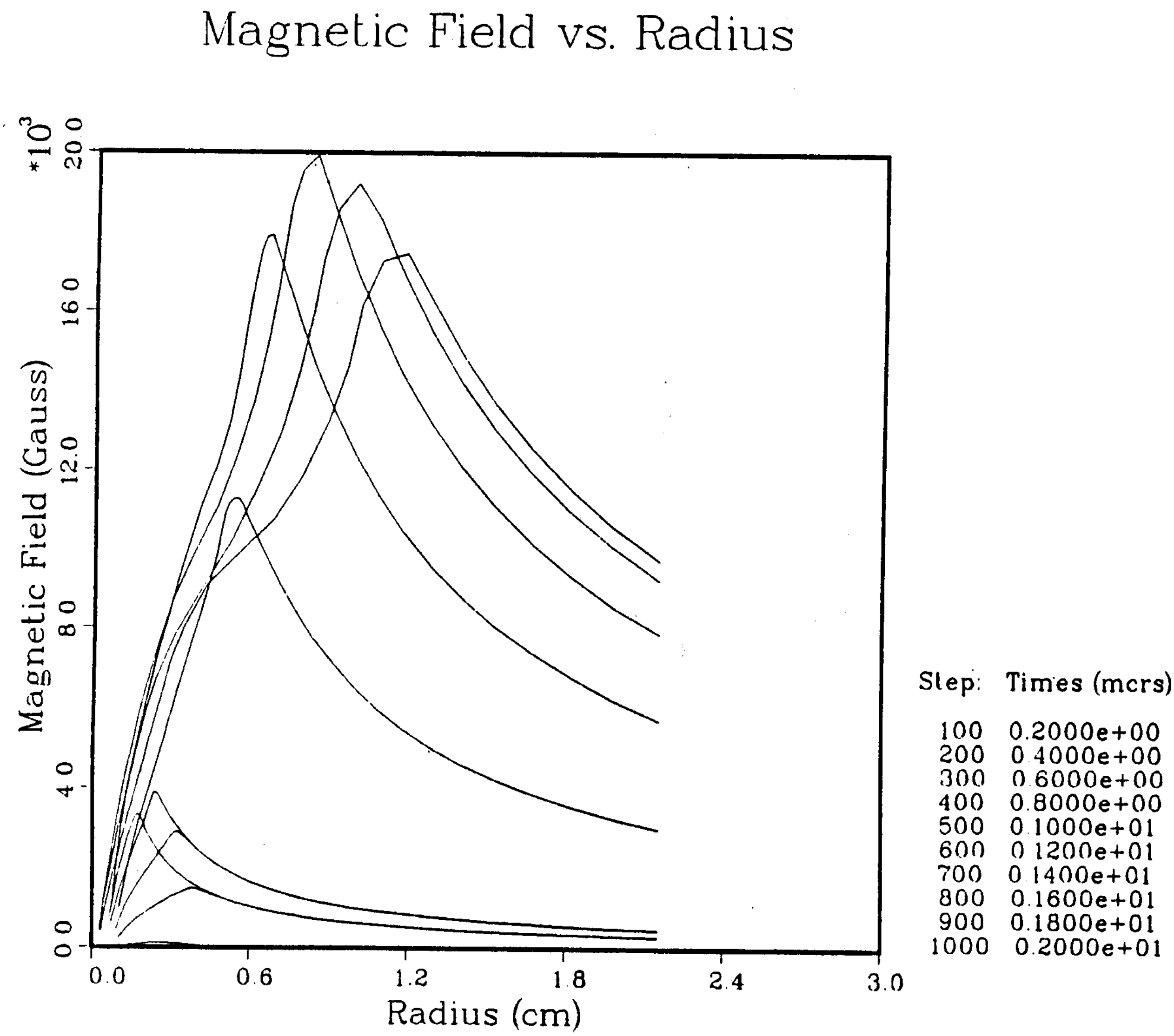

BEST CASE CHANNEL WITHOUT RADIATION

$\Delta T = 1\ \mu s$, Laser Width = 2 mm
Gas = $3.55 \times 10^{17}\ cm^{-3}$ Ar + 0.2% Li

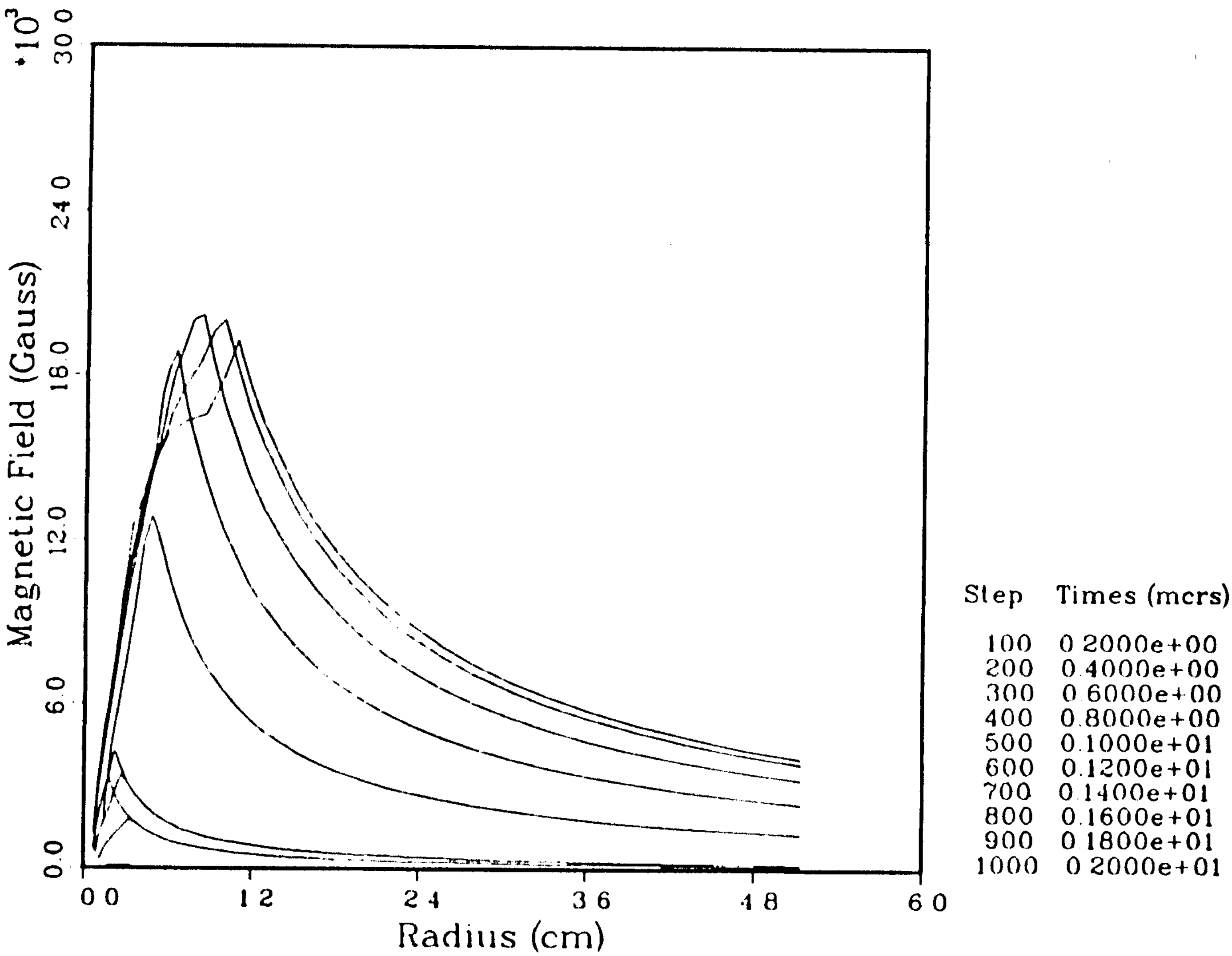

BEST CASE LIBRA CHANNEL WITH RADIATION

$\Delta T = 1\ \mu s$, Laser Width = 2 mm
Gas = $3.55 \times 10^{17}\ cm^{-3}$ Ar + 0.2% Li

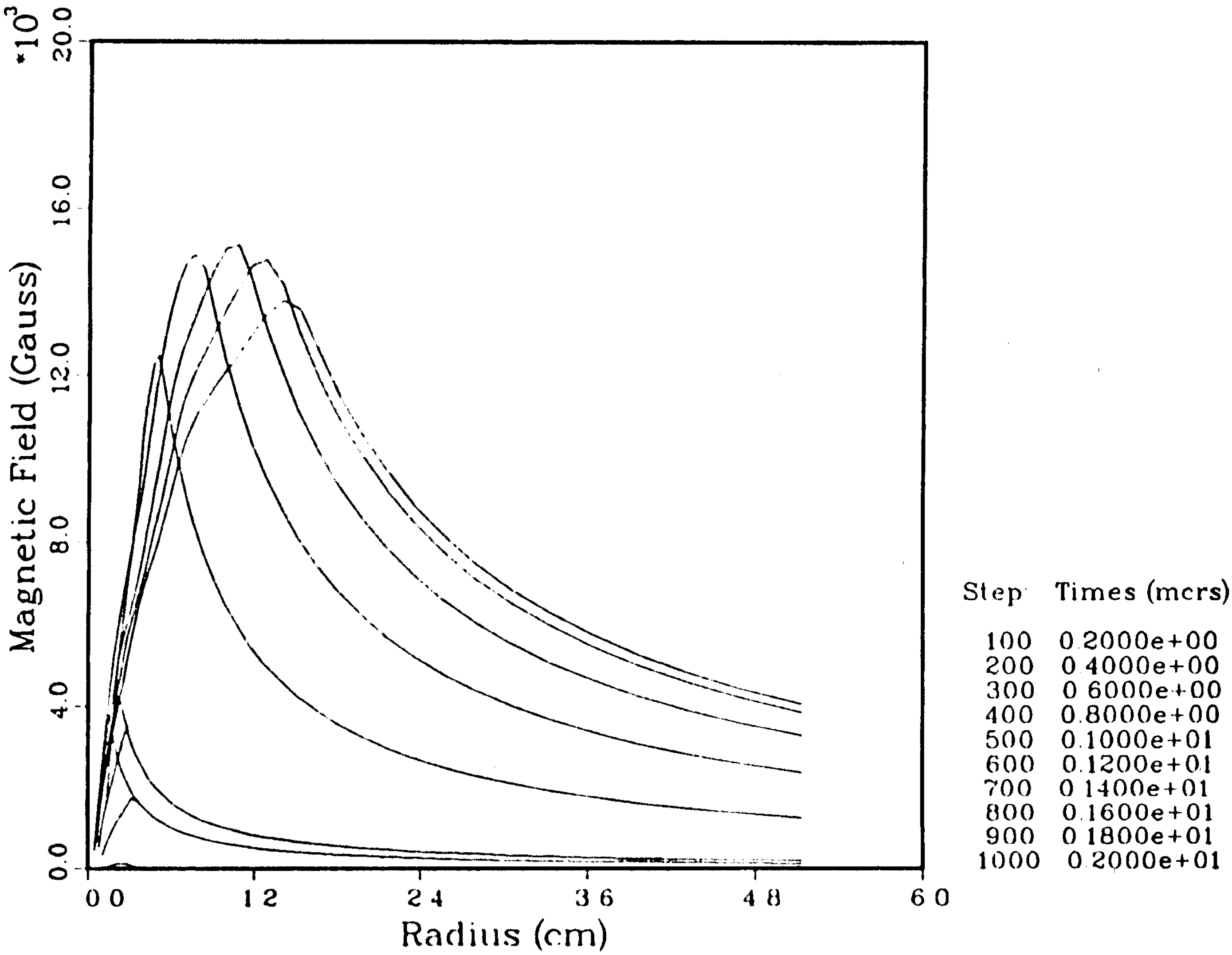

TEMPERATURE PROFILES IN LIBRA CHANNELS

Without Radiant Heat Transfer

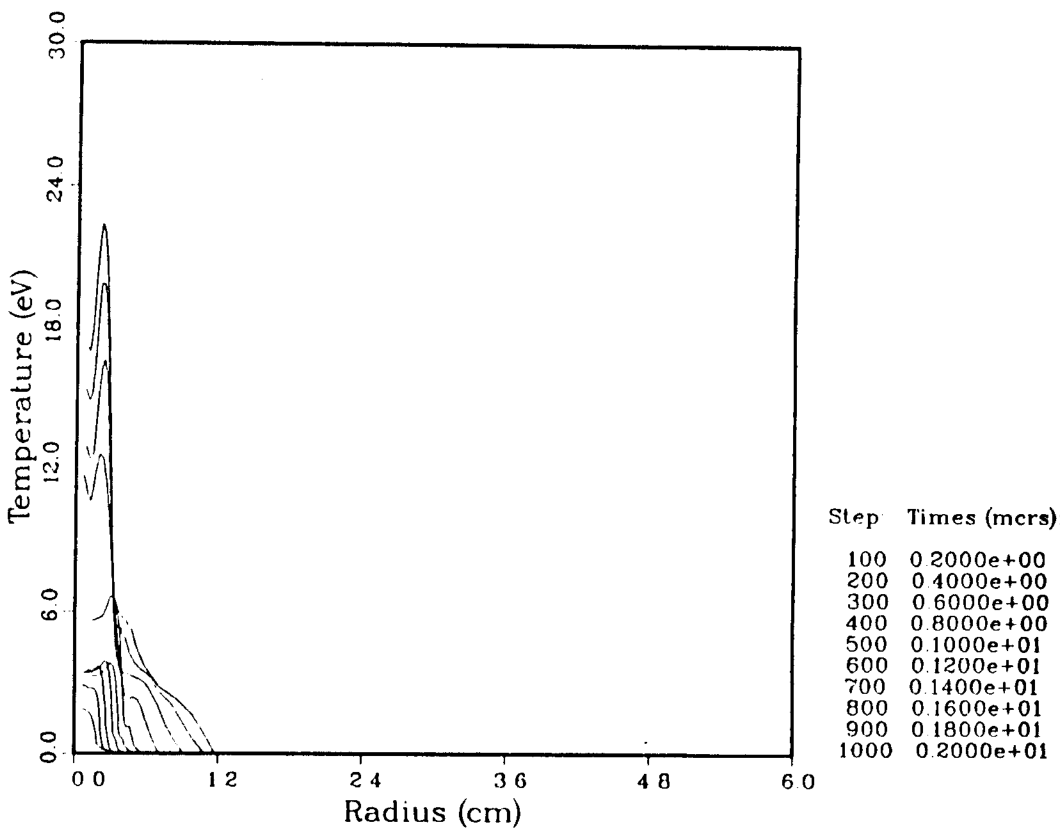

With Radiant Heat Transfer

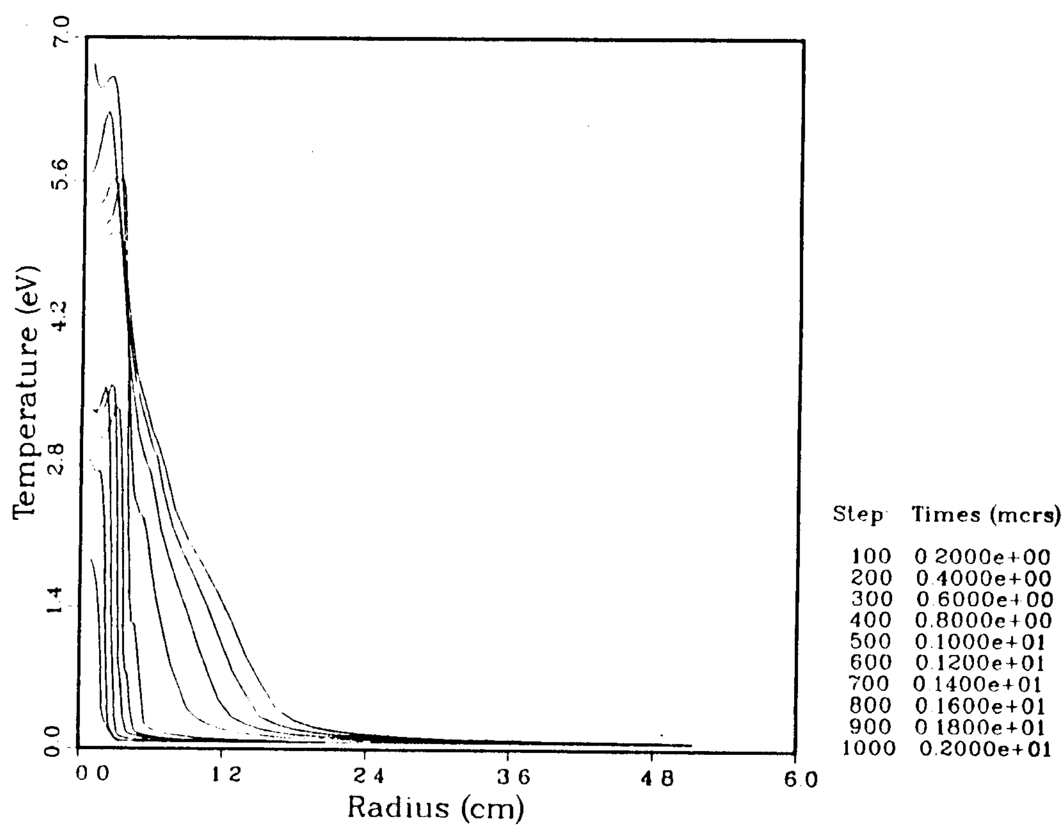

Radiation Transport is Important Issue for LIBRA Channels

- Radiant heat transfer can spread out hot region of channel, where electrical conductivity is high.

- This spreading causes discharge current to flow in a cylinder of larger radius than if there were no radiation.

- Any current that flows more than 0.5 cm from the channel axis is "wasted" because it only creates magnetic field more than 0.5 cm from the channel axis.

- Therefore, radiant heat transfer can reduce the magnetic field 0.5 cm from the channel axis, which is the place that the amplitude of magnetic field needs to be high.

- From comparisons of radiant heat transfer, as calculated with the radiation diffusion method, with small blast experiments we believe that ZPINCH might overestimate the radiant heat transfer in channels.

Is the Current History Realistic?

- Inductance of channel is at least 1 μH per meter of channel length

$$L_{\text{channel}} = 2 \; x \; 5.4 \text{ meters } x \; 1 \; \mu\text{H/m}$$

$$= 10.8 \mu\text{H}$$

- The maximum current and risetime of the second discharge current pulse leads to $\dot{I} \simeq 10^{11}$ A/s.

- Therefore the voltage required to drive this current pulse is

$$V_D = L\dot{I} = 1 \text{ MV}$$

- Can such a large electrical potential only cause a discharge down the length of the channel and not to some other structure? We do not know.

Conclusions

We have discussed:

1) **Channel parameters for LIBRA and have compared them with EAGLE and TDF**

2) **Optimization of channels in N_2 gas (relevant to TDF)**

3) **Channel simulations in Ar + 0.2% Li for LIBRA**

4) **The importance of radiation in channels**

5) **The problems of providing the required current history.**

The present status of channels in LIBRA is:

1) We have a design that provides a 20 kG magnetic field 0.5 cm from the channel axis, if radiation can be neglected. This should be compared to a design goal of 28 kG.

2) If our radiative diffusion calculation is correct we have only 14 kG.

3) We don't yet know what problems the high discharge voltage will cause.

Recommendations:

1) We should continue optimizing the channel design–but with a new version of ZPINCH that may better predict the radiation.

2) The high discharge voltage problem must be considered.

30 MV Accelerator Design
(viewgraphs available under separate cover)

Heating of the Target During Injection

- The cryogenic DT fuel must be in a symmetric hollow shell at liquid or solid density when the driver fires.

- Convective and radiant heat from the target chamber and frictional heating by the injector gun barrel can warm the target.

- We have calculated the temperature in target with a finite–difference heat transfer computer code with temperature–dependent thermal properties.

- We will present:

    1) Limits on the fuel temperature

    2) Heating of the target during acceleration in gun

    3) Heating of the target while in target chamber

    4) Conclusions

Limits on Fuel Temperature in Cryogenic Targets

- **Solid DT fuel**

$$T_{fuel} < 19.7 \text{ K (triple point for DT)}$$

- **Liquid DT held in place by a low density rigid foam**

  T_{fuel} can be as high as 30 K, depending on the acceptable DT vapor density in capsule center.

LIBRA Target is in Sabot in Gun Barrel but Bare in Target Chamber

LIBRA Target Moving Through Target Chamber Gas

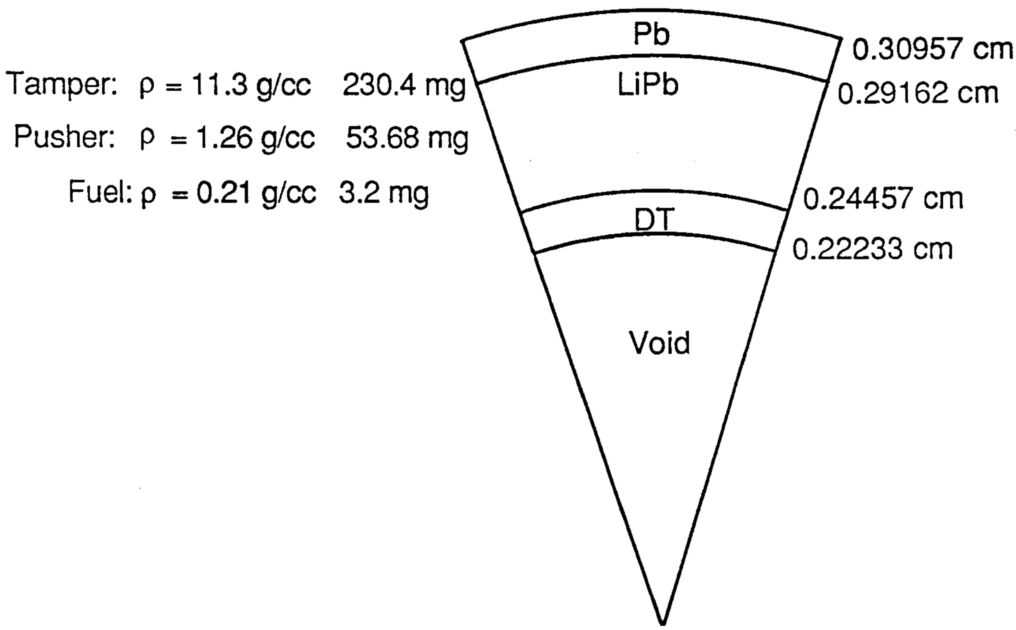

Target in Sabot in Gun Barrel

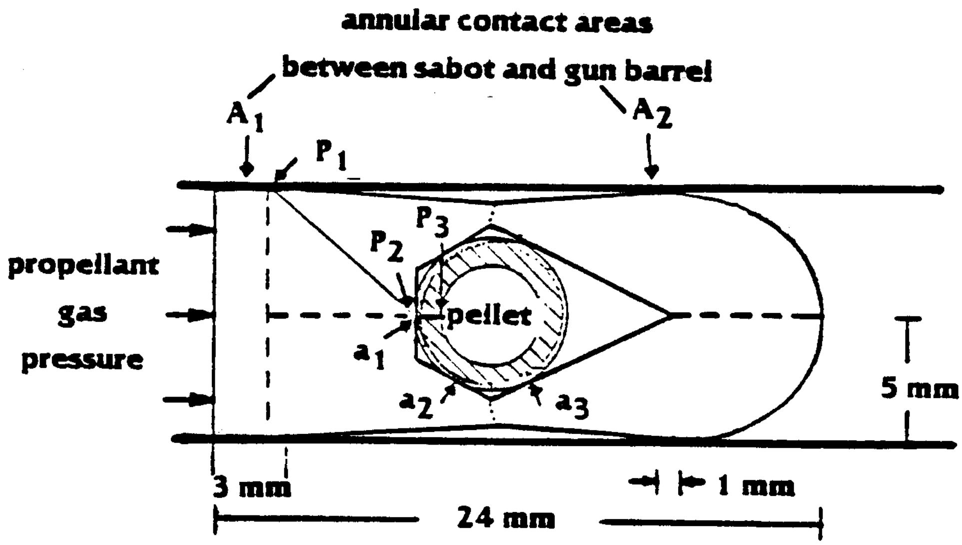

Sabot Protects Target from Heating During Acceleration

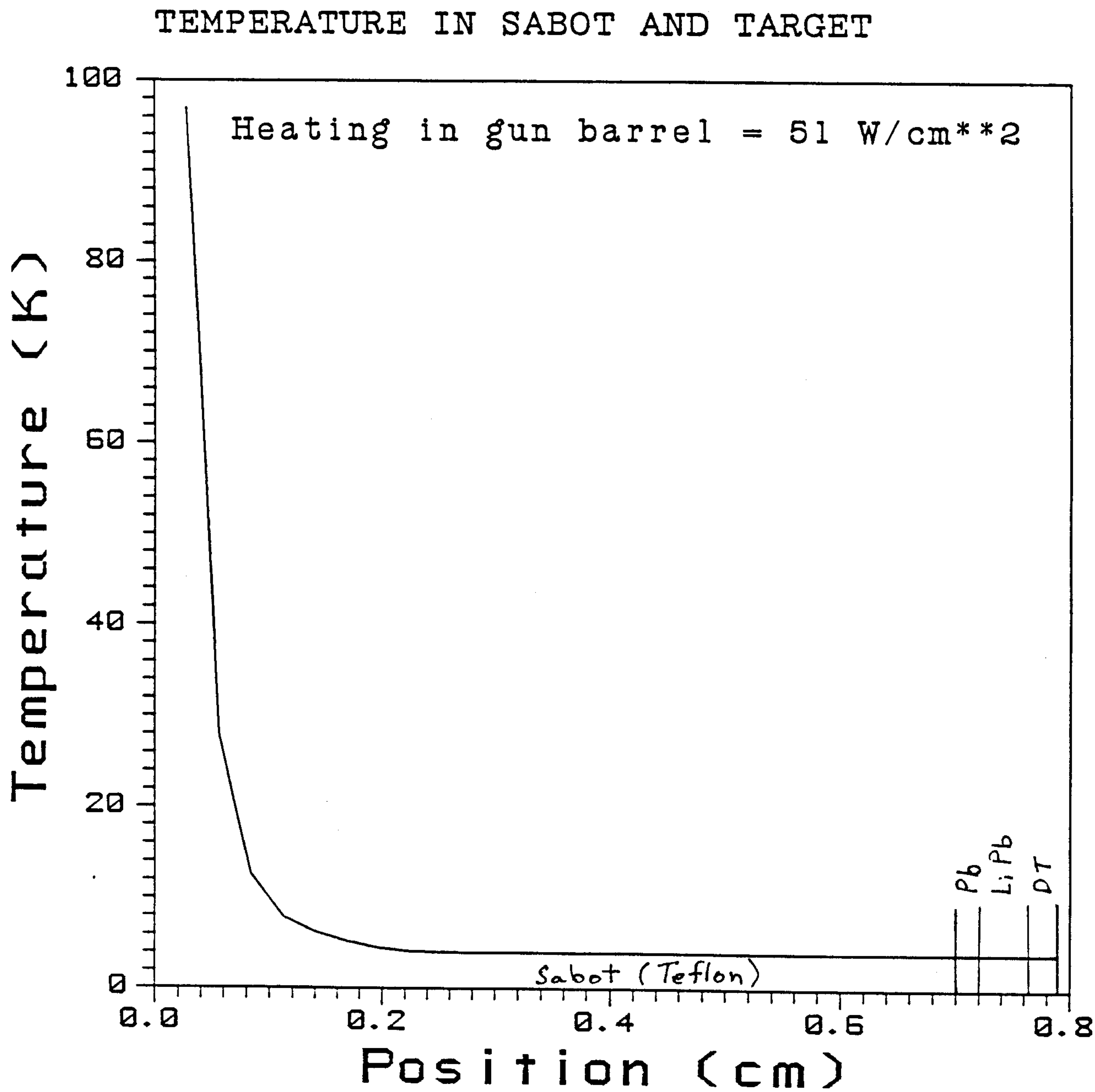

Heat Loads in Target Chamber Gas

Convective Heat Transfer

Parameters

$T_{gas} = 800$ K
$V_{target} = 200$ m/s
$d_{target} = 1$ cm
$\rho_{gas} = 2.4\text{x}10^{-5}$ g/cm^3
$t_{injection} = .025$ s
$\mu_{gas} = 480\text{x}10^{-6}$ g/cm-s

$$Re = \frac{V d \rho}{\mu} = 985$$

$$Nu = \frac{hcd}{kg} = 0.37\ (Re)^{0.6}\quad \text{(Kreith)} \qquad = 23$$

k_f = thermal conductivity of gas = $1.9\text{x}10^{-4}$ W/cm-K
h_c = surface conductance = $4.3\text{x}10^{-3}$ W/cm^2-K

$$\ddot{q}_{conv} \simeq h_c T_{gas} = 3.5\ \text{W/cm}^2$$

Radiative Heat Transfer

$$\ddot{q}_{rad} = 5.7\text{x}10^{-12}\ \text{W/cm}^2\ T_g^4$$
$$= 2.0\ \text{W/cm}^2$$

Total

$$\ddot{q}_{total} = 5.5\ \text{W/cm}^2$$

Target is Heated in Target Chamber

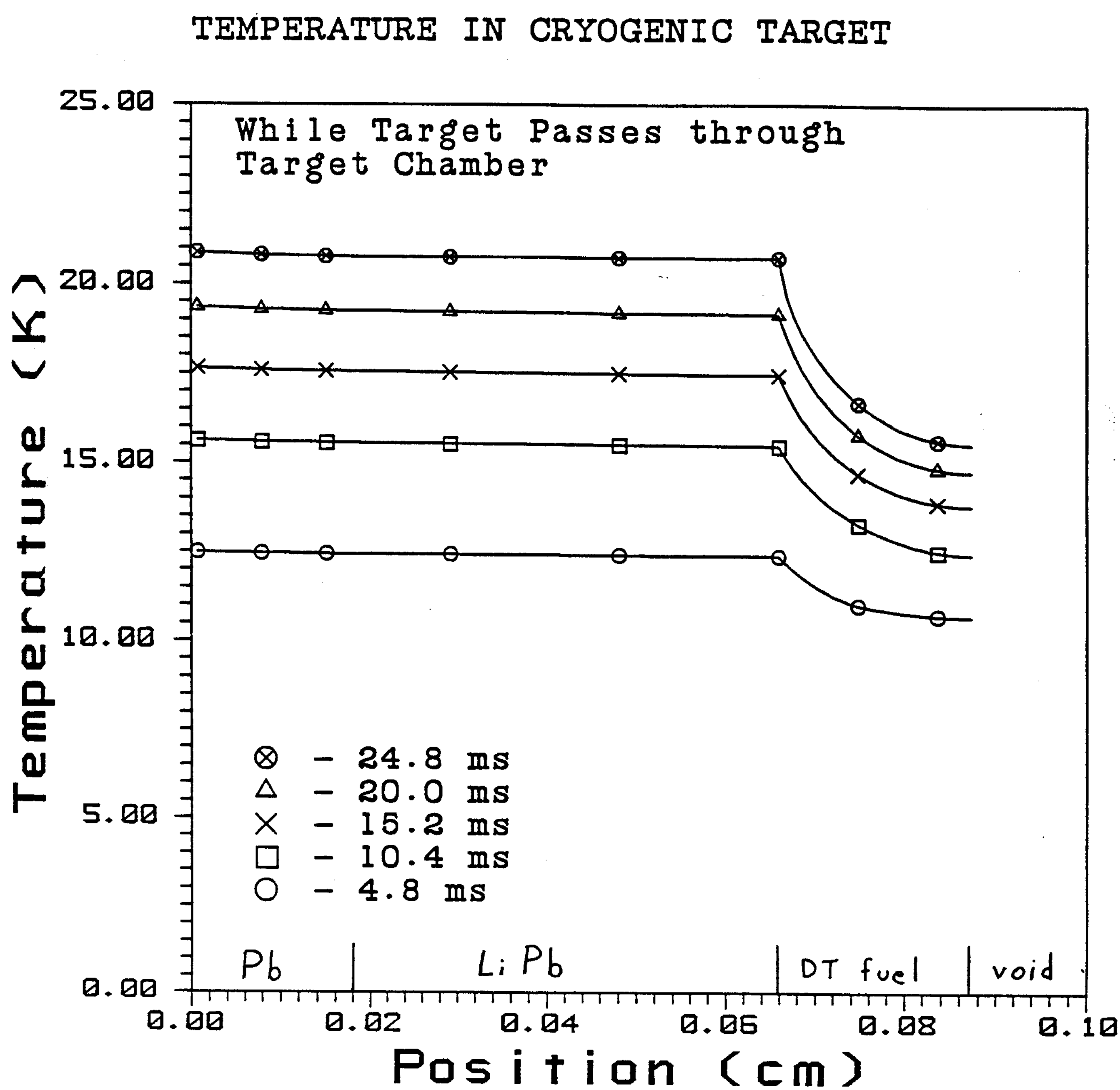

The Heat Transfer is Not Uniform Around the Target

Pattern for a low Re flow about a sphere (from An Album of Fluid Motion by Van Dyke)

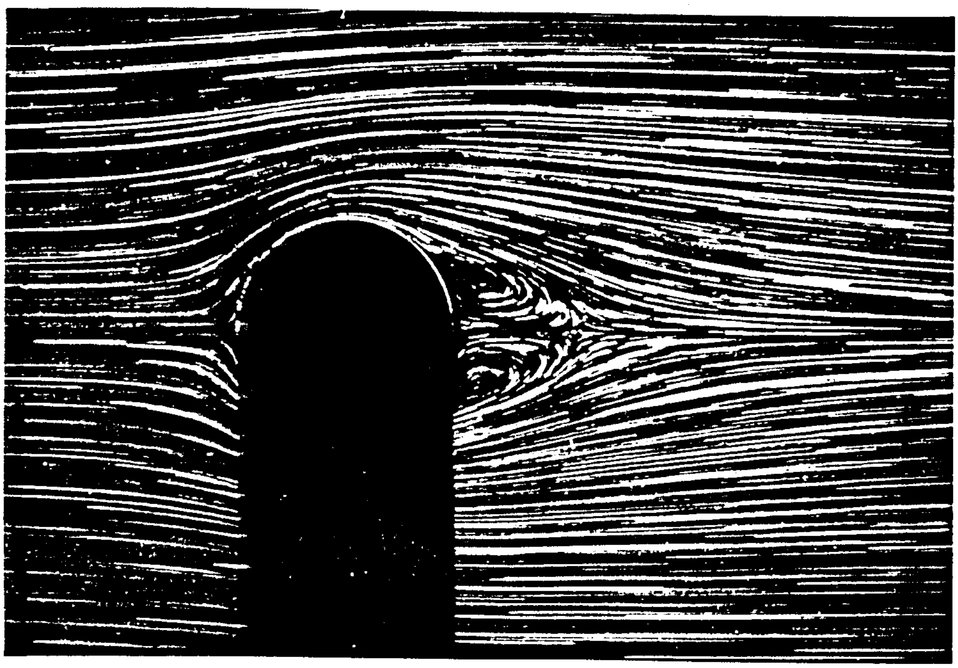

51. Sphere at $R = 56.5$. As in figure 8, the sphere is falling steadily down the axis of a tube filled with oil, but here so large that the influence of the walls is negligible. Magnesium cuttings are illuminated by a sheet of light, which casts the shadow of the sphere. *Archives de l'Académie des Sciences de Paris. Payard & Coutanceau 1974*

Higher heat transfer at stagnation point on leading edge and at vortex ring at back of target.

We have no data for Reynolds numbers as low as 1000 but, from the trends at higher Re, we believe that the variation will be by no more than a factor of 2 from the average.

There may be some thermal smoothing of the temperature in the outer lead shell.

The effects of this nonuniform heat load on the fuel are unknown at this time.

Conclusions

- Sabot protects target during acceleration – target remains at 4 K until entrance to target chamber.

- Cryogenic fuel heats to slightly above 20 K – too hot for solid DT but acceptable for liquid DT in foam.

- Increasing injection velocity will improve situation, but only slowly because $\ddot{q}_{\mathrm{conv}} \propto v^{.6}$.

Cavity Calculations (CONRAD Code)

PURPOSE

1) Calculate the radiation flux and pressure impulse at the INPORT tubes to find the mechanical stress on the tubes and the heating in the LiPb coating.

2) Determine the mass of LiPb vaporized from the INPORT tubes due to the prompt, high energy x-rays and the thermal radiation. This mass must be removed from the cavity gas, either by condensation or pumping, before the next target implosion.

INPUT FOR CALCULATIONS

1) Energy released from target:

231 MJ	(neutrons)
63 MJ	(x-rays)
26 MJ	(ions)
320 MJ	(total)

2) Background gas: argon, pressure = 10 torr

3) Distance to INPORT tubes = 3 m

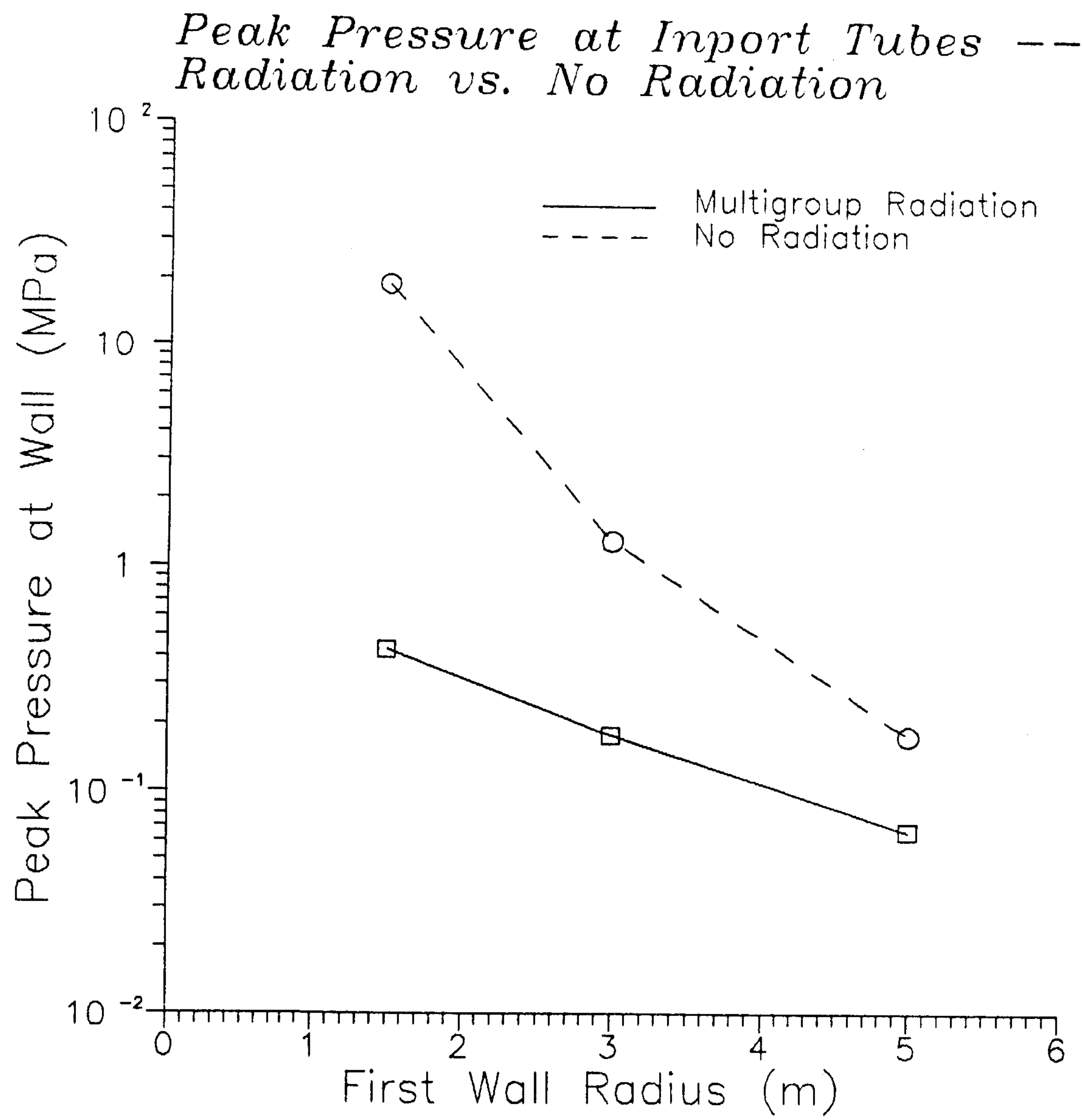

- **Including radiation transport in the calculations significantly reduces the peak pressure of the shock front at the INPORT tubes.**

- **The pure hydrodynamics (no radiation) results provide an upper limit for the peak shock pressure.**

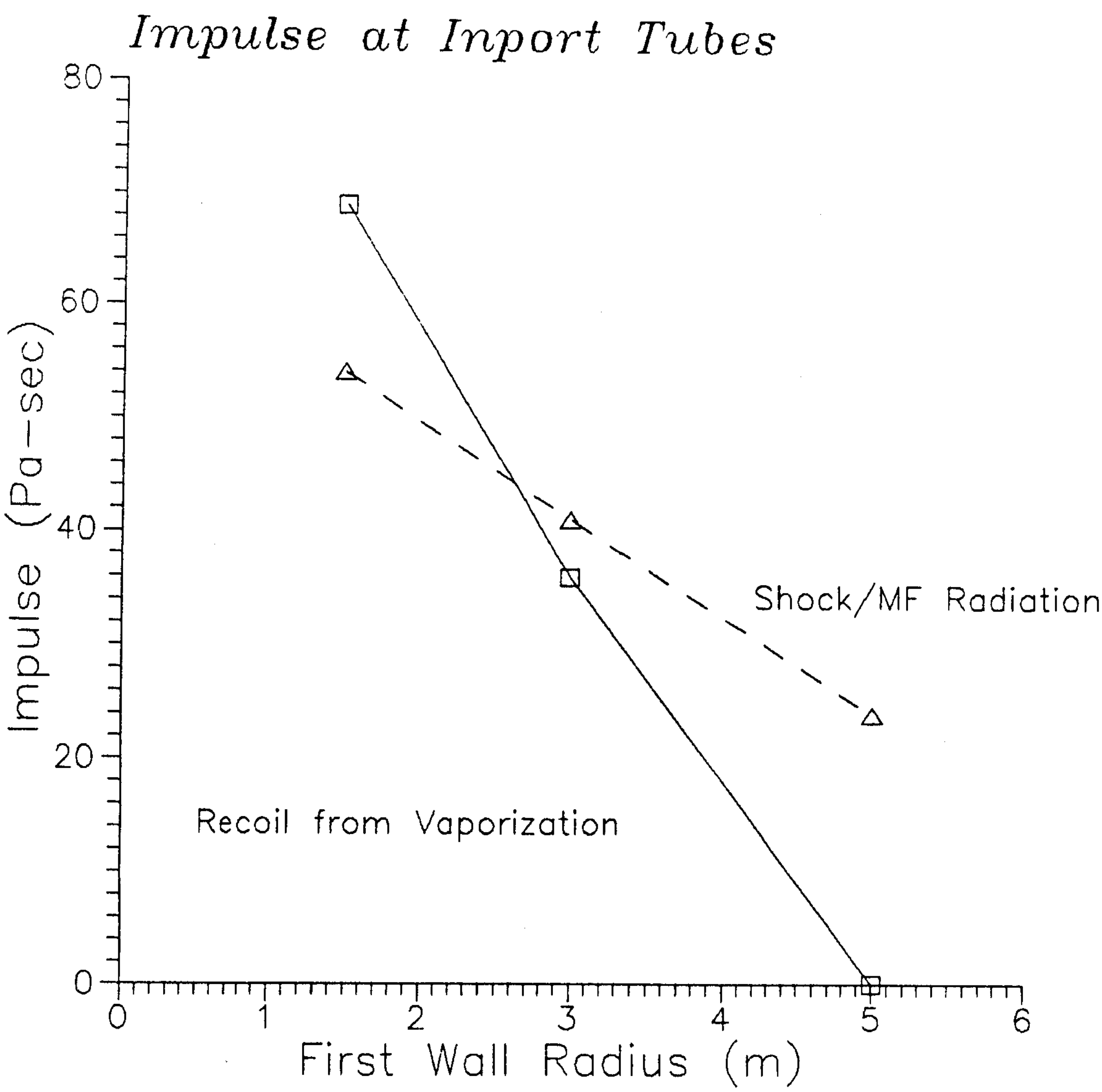

- **The "recoil impulse" from the rapid vaporization of LiPb can exceed the shock–produced impulse when the distance to the tubes is $\leq 2\frac{1}{2}$ meters.**

- **The total impulse on the INPORT tubes at 3 m is about 80 Pa-s.**

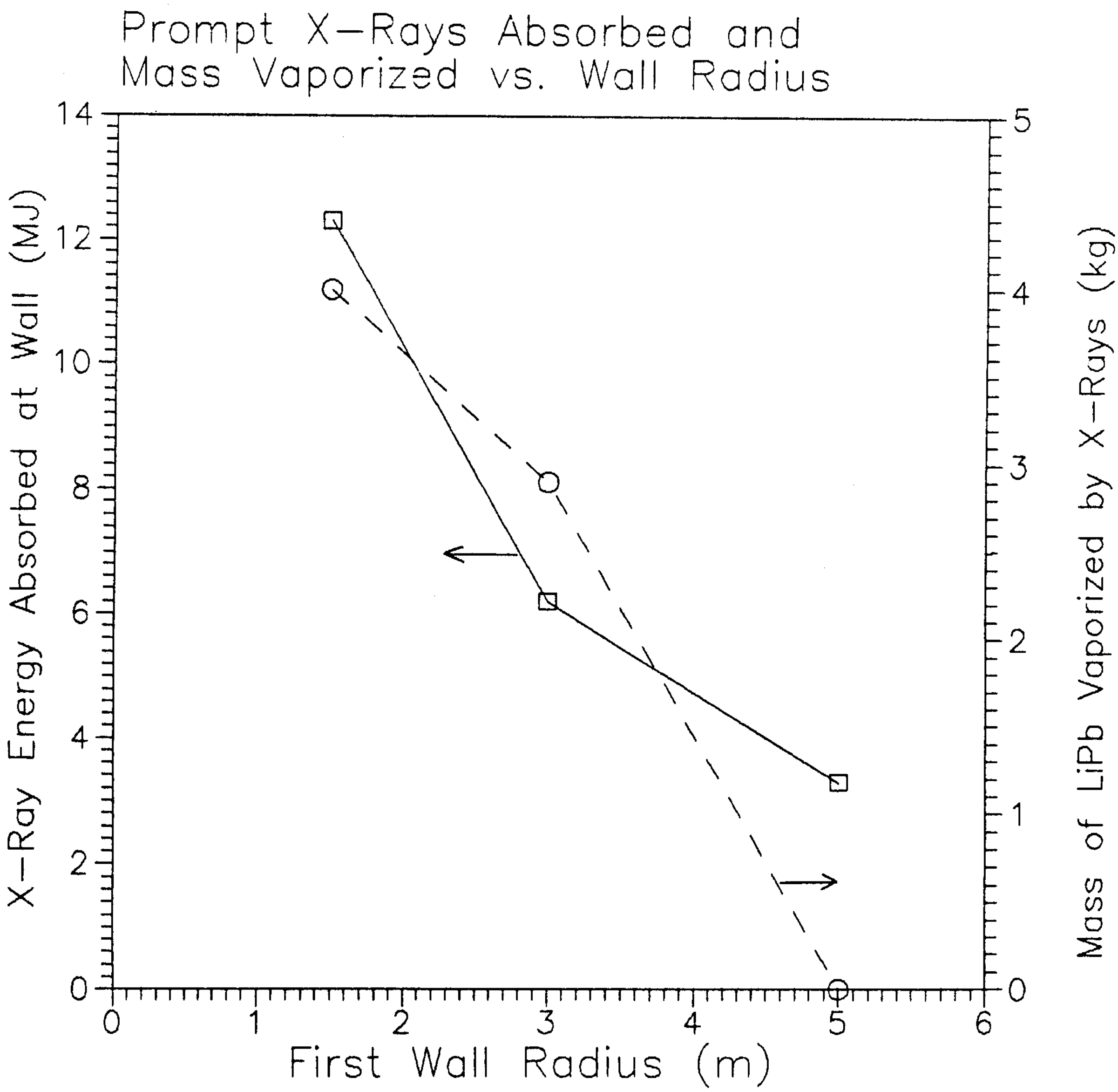

- At a distance of 3 m, roughly 90% of the target x-rays are absorbed by the background gas, so that ~6 MJ are absorbed by the LiPb coating on the INPORT tubes.

- The mass of LiPb vaporized by the target x-rays is 2.9 kg. By comparison, the original cavity gas mass is 2.7 kg.

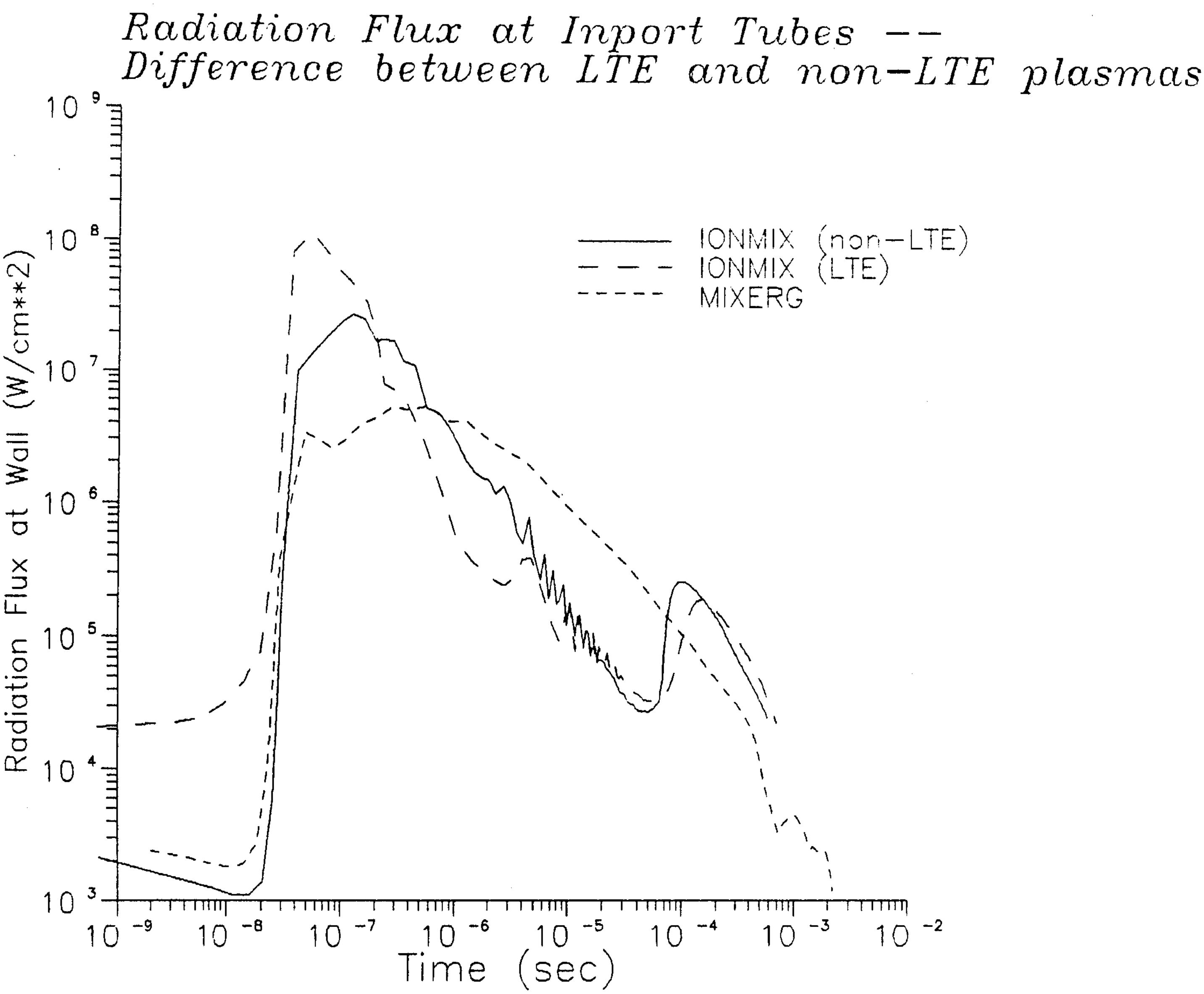

- We have developed a new equation of state and opacity code (IONMIX) that calculates the radiative properties of both LTE and non-LTE plasmas.

- The assumption of LTE leads to overestimating the radiative flux at the tubes at early times ($\leq 0.2\ \mu s$), and underestimates the flux at later times. (The solid line is expected to be the most accurate curve.)

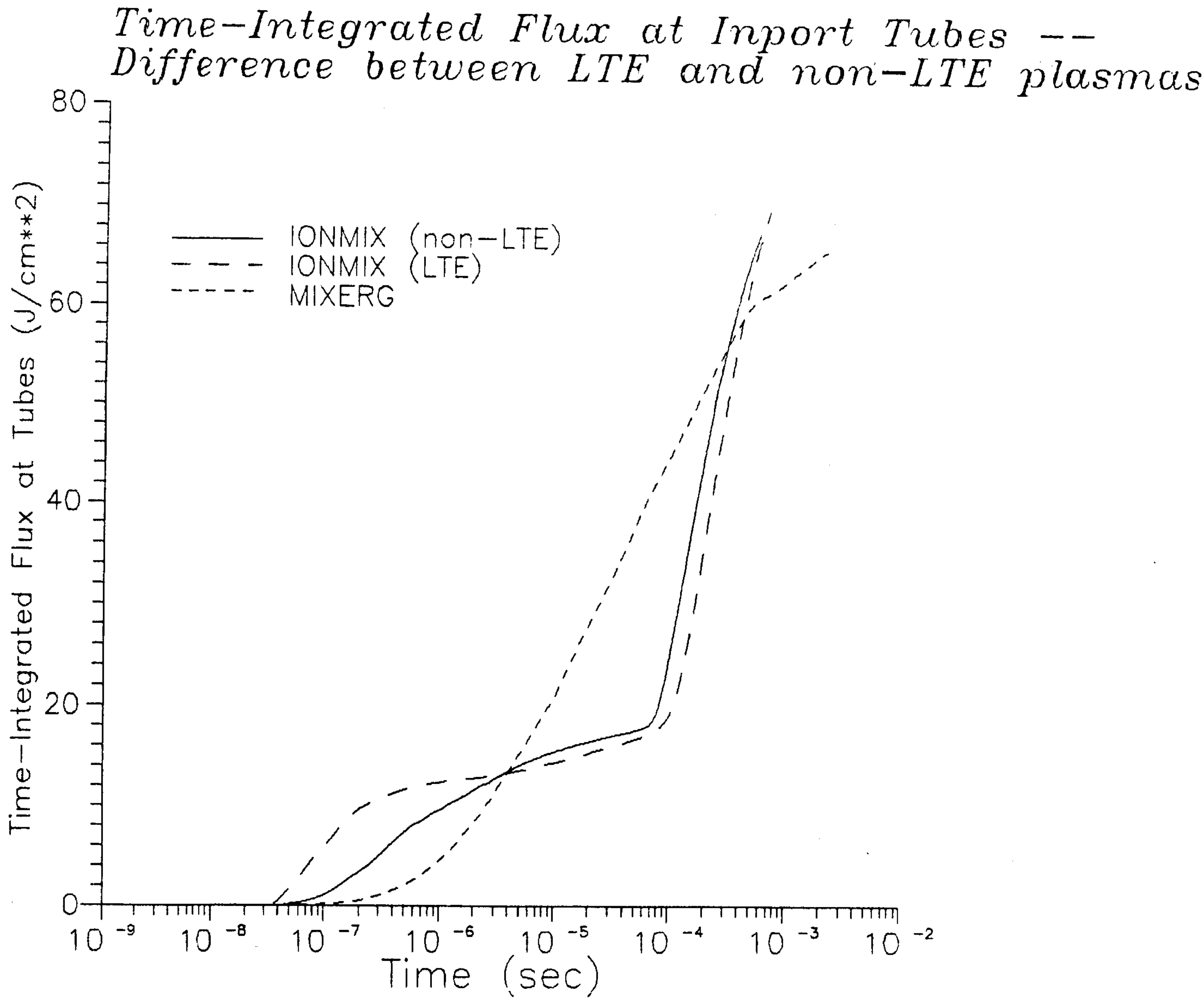

- **Roughly 1/4 of the x-ray and ion energy is radiated to the INPORT tubes before the shock arrives at the tubes ($t_{SHOCK} \approx 0.3$ ms).**

- **Non-LTE effects are noticeable when the background gas pressure is 10 torr, and become even more important at lower pressures.**

Features of the CONRAD Radiation–Hydrodynamics Code

- One dimensional, one fluid lagrangian hydrodynamics with Von Neuman artificial viscosity

- One temperature plasma approximation ($T_{electron} = T_{ion}$)

- Multifrequency (20 group) flux limited diffusion of radiation

- Equation of state and opacities based on semi–classical atomic model (MIXERG code)

- Time dependent target point source x-ray attenuation in plasma using Bigg's cross section data

- Time dependent, energy dependent, species dependent, target ion stopping in plasma using combined bound electron, nuclear, and free electron stopping powers (SNL–Mehlhorn model)

Physical Processes in ICF Target Chambers

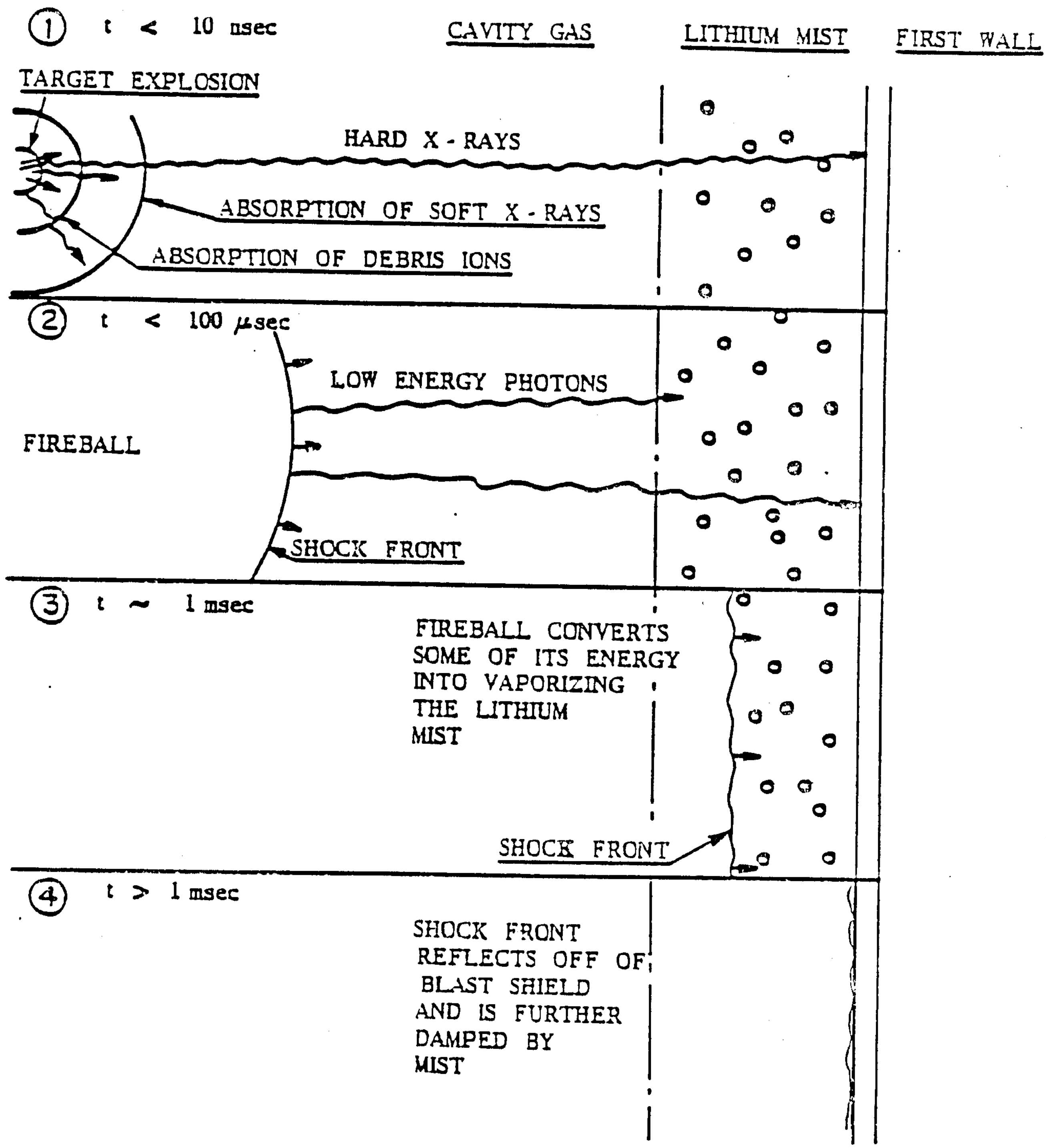

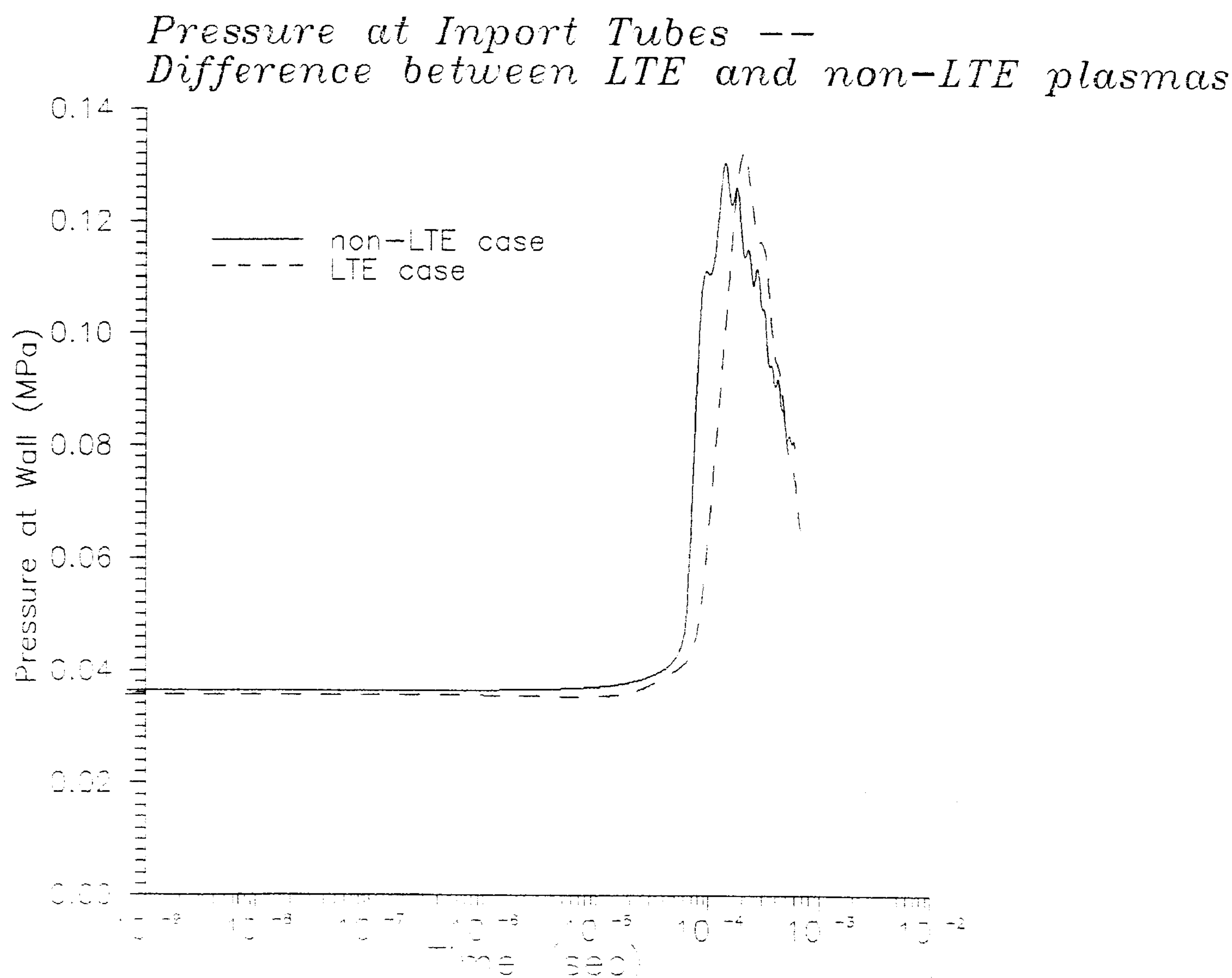
Pressure at Inport Tubes --
Difference between LTE and non-LTE plasmas
non-LTE case
LTE case
Pressure at Wall (MPa)
0.14
0.12
0.10
0.08
0.06
0.04
0.02
0.00
Time (sec)

General Parameters Used to Calculate Required Pumping Speed:

Radius to INPORT tubes (m)	3.0
Radius to Vacuum Wall (m)	5.0
Height from Bottom Pool to Roof (m)	6.0
Volume Fraction in INPORT Zone (%)	33
Gas in Chamber	Argon
Volume of Gas in INPORT Zone (m^3)	202
Volume of Gas in Cavity Center (m^3)	170
Pressure in Chamber Before Shot (torr)	26
Temperature in Chamber Before Shot (K)	800
Pressure in Chamber After Shot (torr)	290
Temperature in Chamber After Shot (K)	9000

Procedure and Assumptions Used to Calculate "LIBRA" Pumping Requirement

- It is assumed that a suppression chamber with LiPb cooling at 623 K is connected to the target chamber. The pressure in the suppression chamber is maintained at 26 torr.

- After the shot the gas in the target chamber expands isentropically into the suppression chamber and the pressure in both chambers equilibrates.

- Temperature of gas in the INPORT tube zone is assumed at 773 K (500°C) while that in the chamber center stays at the isentropic expansion temperature.

- As the temperature in the chamber cools down to 800 K the pressure falls below 26 torr and fresh argon is injected to replace that which was evacuated.

- The gas in the suppression chamber is pumped out until the pressure reaches 26 torr at 623 K.

- Pumping speed is calculated while varying the volume of the suppression chamber and using a rep rate of 3 Hz.

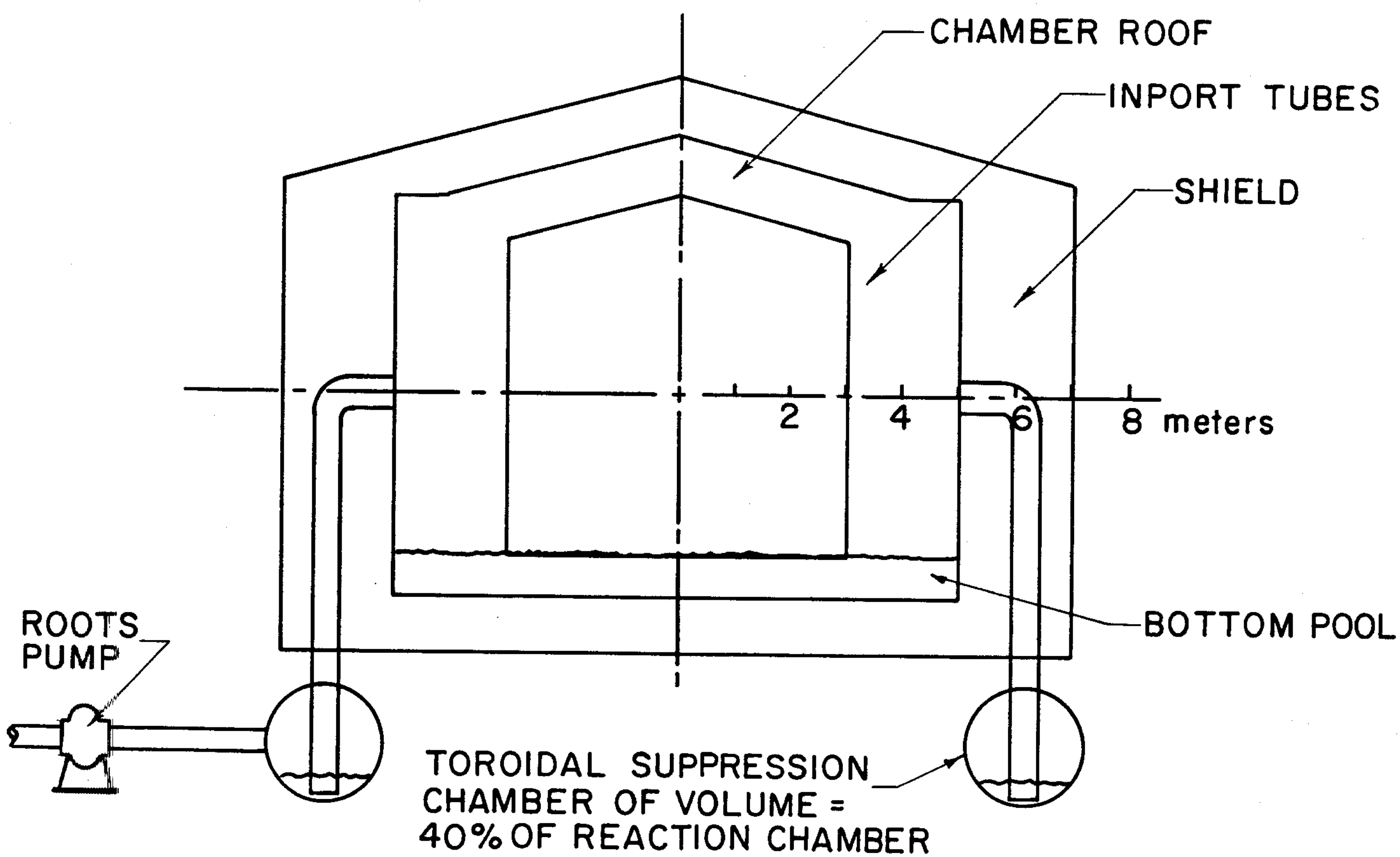

SCHEMATIC CROSS SECTION OF LIBRA CHAMBER WITH A SUPPRESSION CHAMBER SHOWN TO SCALE FOR $V_S/V_T = 0.4$

Pumping Parameters for LIBRA

Ratio of Suppression Chamber Volume to Target Chamber Volume	Gas Temperature In Target Chamber After Isentropic Expansion (K)	Gas Average Temperature in Target Chamber After Equilibrium with Suppression Chamber (K)	Gas Average Pressure in Target Chamber and Suppression Chamber After Equilibrium (torr)	Ratio of Pressure After Equilibrium to Steady State Pressure	Fraction of Target Chamber Gas Mass Exhausted per Shot (%)	Pumping Speed Required (l/s)
1.0	1440	1076	29	1.12	16.4	1.23×10^5
0.8	1652	1173	30.8	1.47	19.3	1.53×10^5
0.5	2193	1420	35.2	1.76	23.4	1.80×10^5
0.4	2496	1557	38.2	1.95	24.4	1.78×10^5
0.3	2955	1767	42.9	2.21	25.3	1.70×10^5
0.2	3628	2052	50.3	2.57	24.4	1.47×10^5
0.1	4950	2647	68	2.60	21	1.08×10^5

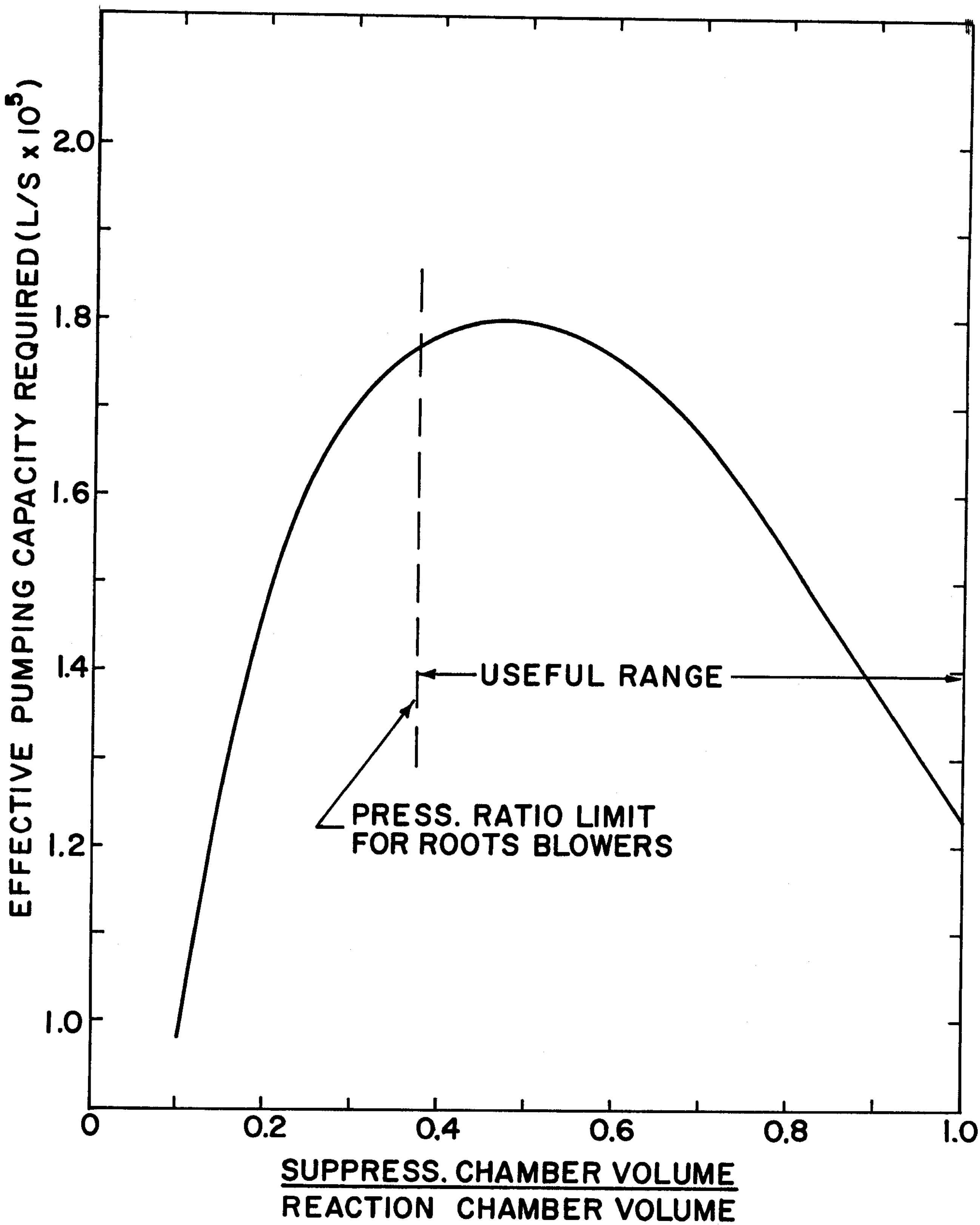

EFFECTIVE PUMPING REQUIREMENT FOR LIBRA
AS A FUNCTION OF SUPPRESSION CHAMBER VOLUME

Results and Conclusions

- A pressure ratio of ≥ 2 is not recommended for roots blowers for sudden pressure fluctuations as is the case in LIBRA. This limits the operation to a range of suppression chamber to target chamber volume ratio of ≥ 0.4.

- As the suppression chamber/target chamber volume ratio decreases, the pumping requirement increases, peaking at V_S/V_T=0.5.

- The most cost effective system trades the price of the suppression chamber with the cost of increased pumping.

- An effective pumping speed of $< 2\text{x}10^5$ ℓ/s and $> 1.2\text{x}10^5$ ℓ/s is required for the LIBRA target chamber, depending on the size of the suppression chamber.

STATUS OF LIBRA NEUTRONICS

Mohamed Sawan

Fusion Power Associates

28–29 January 1988

LIBRA neutronics activities carried out during the last year (1987) are summarized below.

1) **Neutronics benchmark calculations**

   One-dimensional calculations have been performed for different blanket designs by FPA (using ONEDANT) and KfK (using MCNP) and results compared.

2) **Target neutronics calculations**

   Neutronics calculations have been performed for the 3.2 mg LIBRA target to determine the energy spectra of emitted neutrons and gamma photons as well as the breakdown of neutron, gamma, x-rays, and debris yields.

3) **Chamber neutronics analysis**

   One-dimensional neutronics analysis has been performed for the LIBRA chamber to determine design options that satisfy the tritium breeding and wall protection requirements.

Neutronics Information Sent to KfK

Date	Item
2 July 1987	Nuclide densities in blanket and reflector
15 July 1987	Target spectrum used for benchmark calculations
20 July–26 Nov. 1987	10 communications related to benchmark
2 October 1987	Target geometry, composition, and results of target neutronics

Neutronics Benchmark Calculations

- Neutronics calculations performed by FPA using the ONEDANT code, P_3-S_8 approximation, spherical geometry, 30 n–12 γ group cross section data based on ENDF/B-V, and the HIBALL target spectrum. Ten different cases were analyzed using different blanket thicknesses (Δ_B), different reflector thicknesses (Δ_r) and different lithium enrichments ($\%^6$Li).

University of Wisconsin-Madison

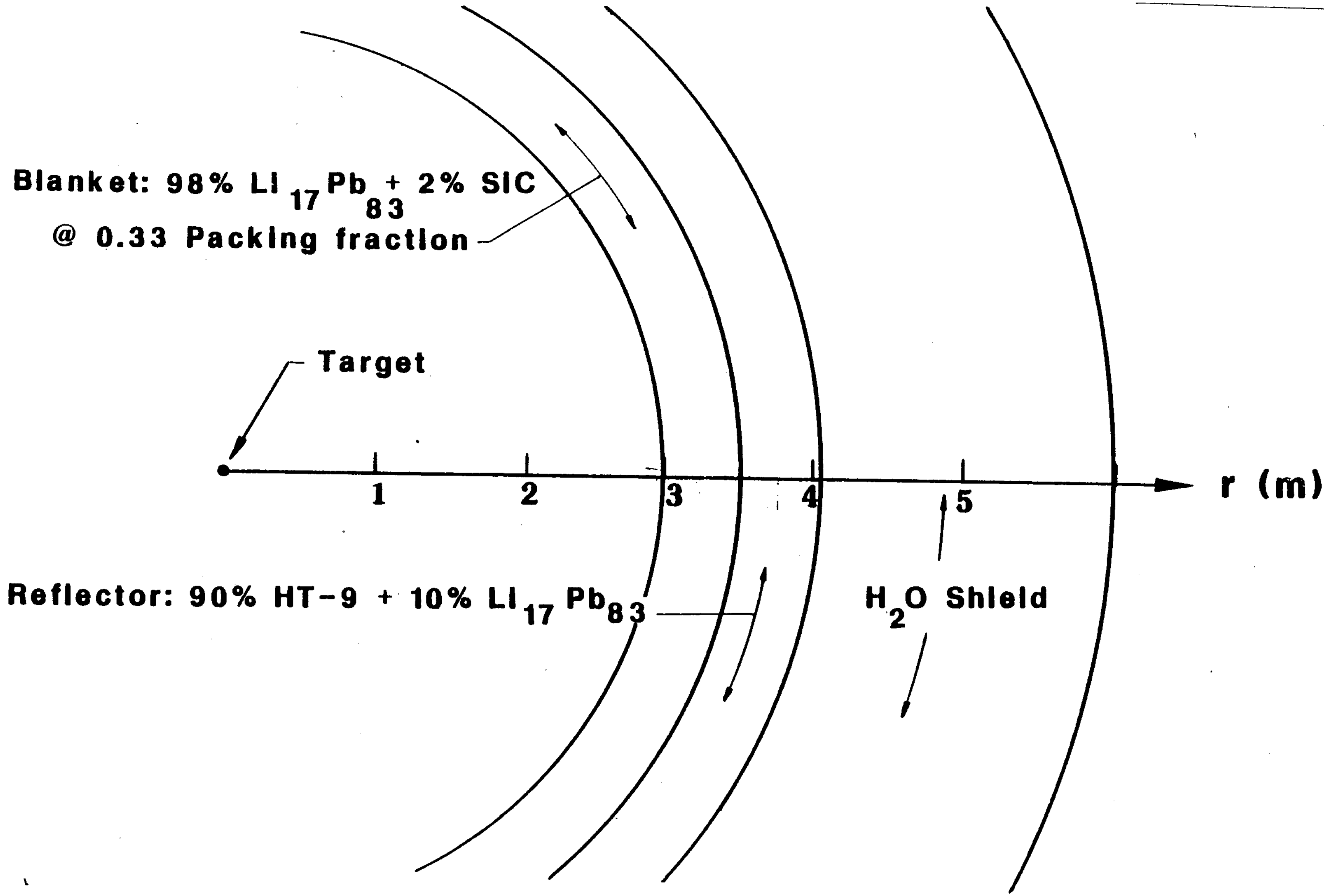

SCHEMATIC OF NEUTRONICS CALCULATIONAL MODEL

Nuclear Parameters Calculated by FPA for the 10 Cases

Case	Δ_B (m)	Δ_r (m)	%^{6}Li	TBR	M_n	M^*_o	Peak HT-9 dpa/FPY
1	2	.5	7.42	1.152	1.366	1.250	2.44
2	2	.5	90	1.625	1.259	1.174	1.21
3	1.5	.5	7.42	0.957	1.407	1.280	5.37
4	1.5	.5	90	1.659	1.278	1.189	3.12
5	1.0	.5	7.42	0.715	1.451	1.312	11.63
6	1.0	.5	90	1.406	1.293	1.200	7.95
7	1.0	.5	35	1.168	1.346	1.237	9.89
8	0.55	.5	90	1.162	1.309	1.211	18.00
9	1.0	.8	35	1.175	1.377	1.258	9.71
10	0.55	0.85	90	1.177	1.374	1.238	17.61

$$M_o = \frac{(0.28 + 0.72M_n)0.99E_{DT}}{E_{DT}}$$

- Tritium breeding ratio calculations have been performed by KfK for cases 2, 4, 6, 8, and 10 using the MCNP version 3 code and different MCNP continuous energy cross section libraries available to KfK. The geometrical model, nuclide densities, target spectrum used are identical to those used by FPA. Analog Monte Carlo was used with no variance reduction method. The E-mail service was used to efficiently compare results and exchange comments between FPA and KfK.

Comparison Between TBR Results Obtained by FPA and KfK

Case	FPA ONEDANT Results	KfK MCNP Results 23 July 87	1 Nov. 87	12 Nov. 87
2	1.625	1.659	1.670	—
4	1.549	1.580	1.591	1.570
6	1.406	1.427	1.442	1.409
8	1.162	1.159	1.193	1.138
10	1.177	1.245	1.254	1.173
Comments	Used as reference for comparison.	Results agree to within 2% except for case 10 the difference is 5.5%. This appears to be due to an overestimate of T_2 production in the reflector (27% higher than case 8).	Used ENDF/B-IV except for ^{6}Li, ^{12}C, and Si. Results agree to within 2.7% except for case 10 the difference is 6.5%.	Used ENDL85 except for ^{6}Li and ^{7}Li. All results agree to within 2%.

Conclusions

- Differences between TBR values calculated by FPA and KfK are attributed to:
  - Different calculational methods (discrete ordinates vs. Monte Carlo)
  - Different energy treatments for cross sections (multigroup vs. continuous energy)
  - Different cross section data (ENDF/B-V vs. ENDF/B-IV or ENDL85)

- Excellent agreement (<2% difference) is obtained between the ONEDANT results using ENDF/B-V data and the MCNP results using the most recent ENDL85 data.

Target Neutronics Calculations

CODE: ONEDANT

Data: 30 n – 12 γ group structure
ENDF/B-V data

Source: Uniform 14.1 MeV neutron source in compressed DT fuel zone

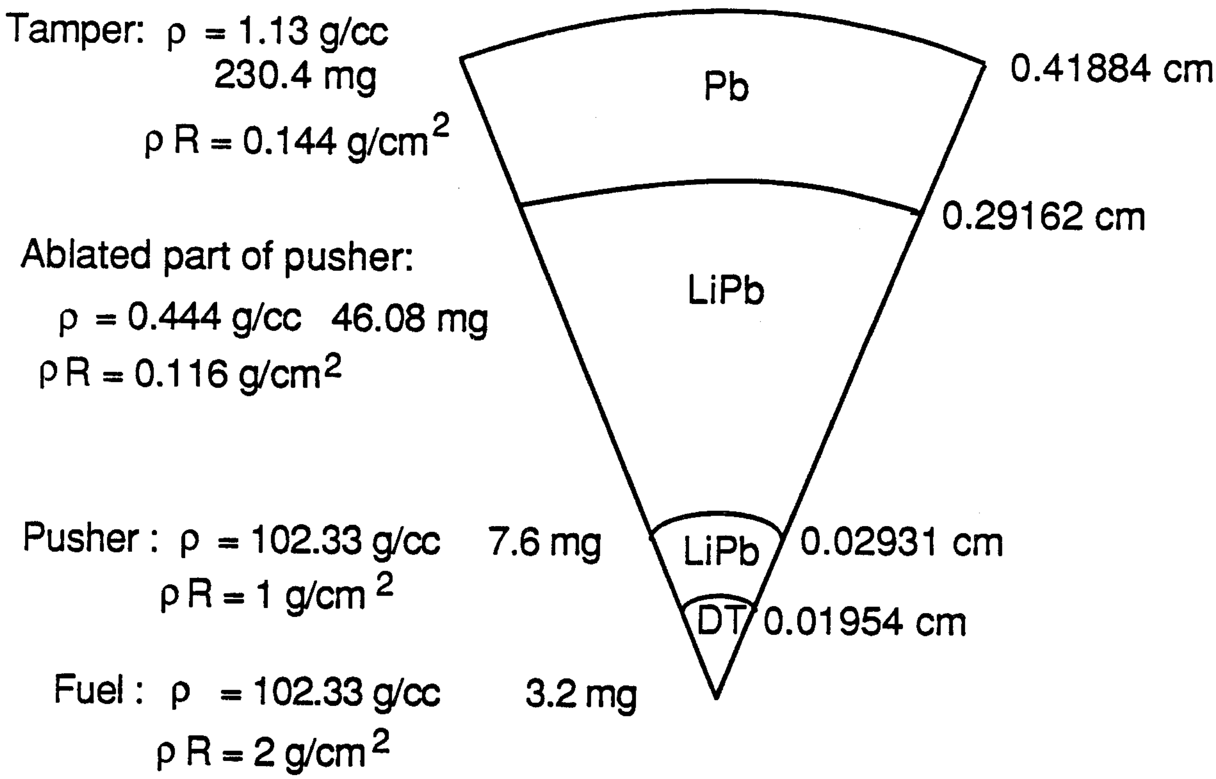

LIBRA Target Configuration at Ignition

Nuclear Energy Deposition in Target

Region	Neutron Energy Deposition (MeV/DT fusion)	Gamma Energy Deposition (MeV/DT fusion)
1	1.1966	1.74×10^{-4}
2	0.1423	1.27×10^{-3}
3	0.0352	1.73×10^{-4}
4	0.0012	2.26×10^{-4}
Total	1.3753	1.84×10^{-3}

Total energy deposited by neutrons and gamma photons in target = 1.377 MeV/DT fusion

Spectra of Neutrons and Gamma Photons Emitted from the Target

Energy carried by neutrons emitted from target	**12.418 MeV/DT fusion**
Number of neutrons emitted from target (70.65% of neutrons at 14.1 MeV)	**1.0285 n/DT fusion**
Average energy of neutrons emitted from target	**12.07 MeV**
Energy carried by gamma photons emitted from target	**0.24 MeV/DT fusion**
Number of gamma photons emitted from target	**0.0168 γ/DT fusion**
Average energy of gamma emitted from target	**1.4 MeV**

Energy lost in endoergic reactions =

$$14.1 - 12.418 - 0.024 - 1.377$$
$$= 0.281 \text{ MeV/DT fusion}$$

ENERGY SPECTRA OF NEUTRONS AND GAMMA PHOTONS EMITTED FROM THE LIBRA TARGET

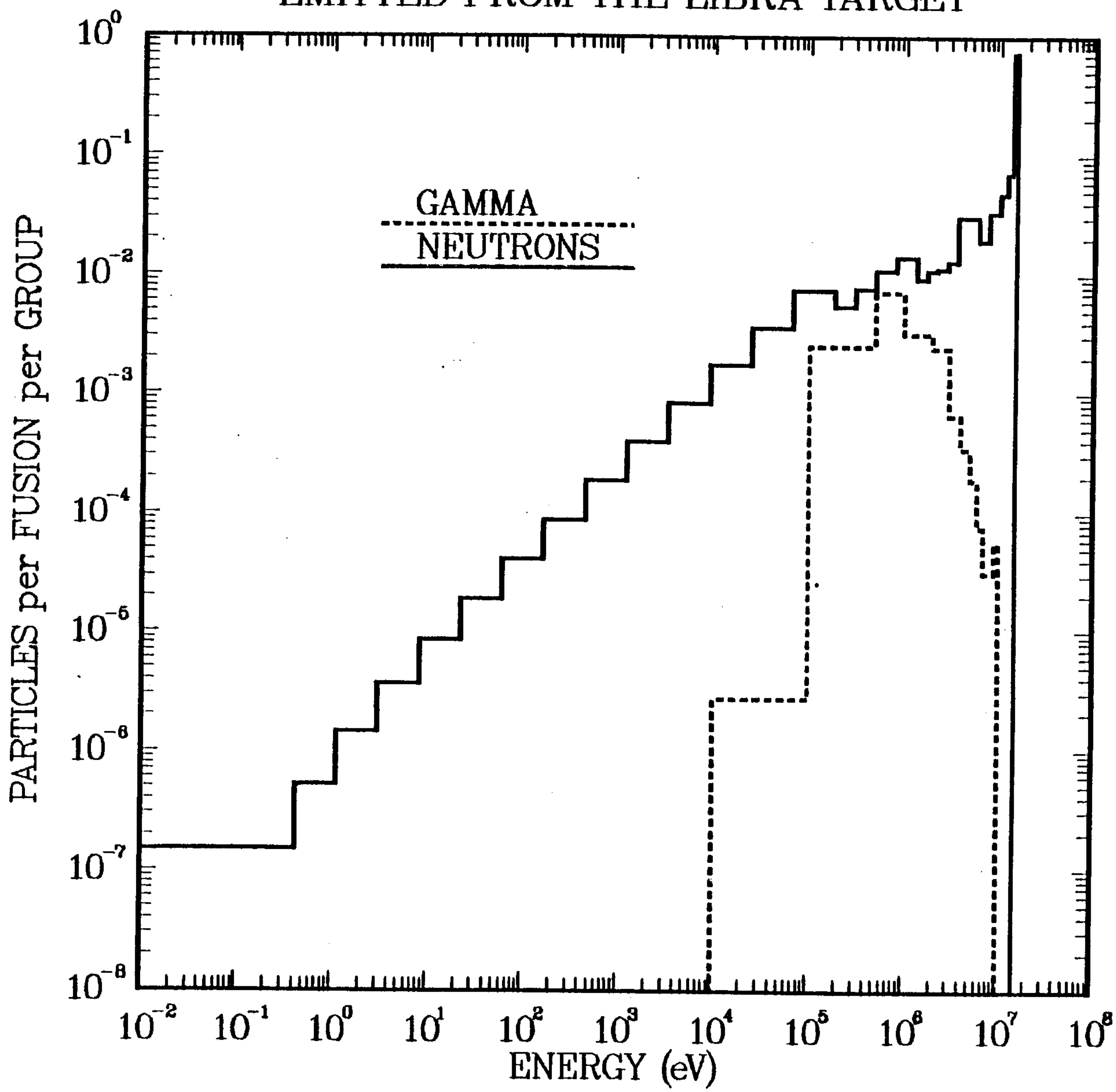

Energy Flow for LIBRA Target

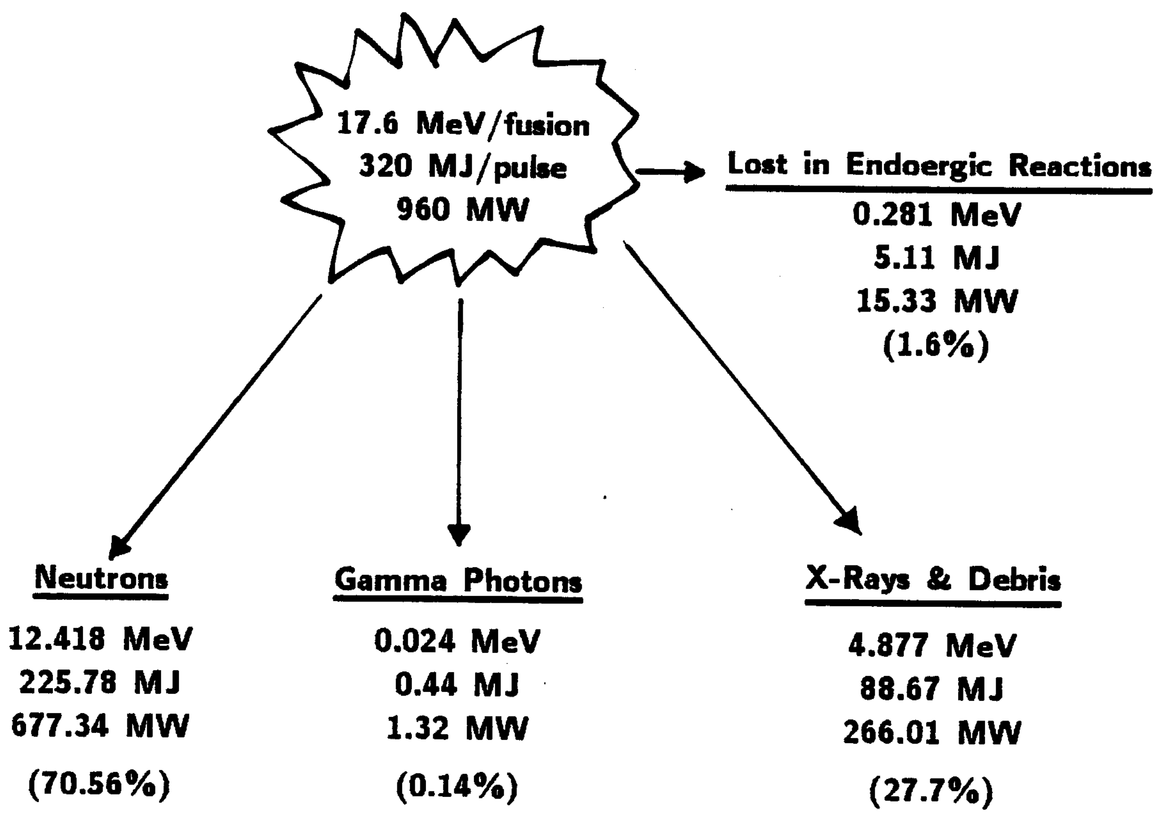

Chamber Neutronics Analysis

- ONEDANT spherical geometry calculations

- 30 n – 12 γ group cross section data based on ENDF/B-V

- Point source at center of chamber emitting neutrons and gamma photons having the spectra calculated for the LIBRA target

- Normalized to 320 MJ DT yield and 3 Hz repetition rate

- Cavity radius = 3 m

- INPORT tubes with 0.33 packing fraction
  2% SiC and 98% $Li_{17}Pb_{83}$ in tubes

- 0.5 m thick reflector consisting of 90% HT-9 and 10% $Li_{17}Pb_{83}$

Design Objectives

- TBR $\geq$ 1.1

- Peak end-of-life dpa in HT-9 $\leq$ 200 dpa. For 30 FPY reactor life the peak dpa rate should not exceed 6.6 dpa/FPY

- Maximize energy multiplication

- Minimize blanket thickness

Design Parameters Varied

Blanket thickness	Δ_B
Lithium enrichment	$\%^6Li$

Case	$\%^6Li$	Δ_B (cm)	TBR	M_n*	M_o**	Peak dpa/FPY in HT-9	Peak He appm/FPY in HT-9
1	7.42	50	0.421	1.465	1.313	38.87	75.46
2	7.42	100	0.705	1.450	1.302	18.40	12.91
3	7.42	150	0.944	1.408	1.273	8.51	2.16
4	7.42	200	1.136	1.366	1.243	3.88	0.37
5	30	50	0.791	1.381	1.253	36.00	75.39
6	30	100	1.108	1.357	1.236	16.07	12.89
7	30	150	1.312	1.323	1.212	6.99	2.15
8	30	200	1.445	1.296	1.193	3.00	0.36
9	90	50	1.108	1.311	1.204	31.16	75.18
10	90	100	1.387	1.294	1.192	12.60	13.57
11	90	150	1.528	1.274	1.178	4.95	2.14
12	90	200	1.603	1.260	1.168	1.92	0.36

*M_n=Nuclear energy multiplication = $\dfrac{\text{Energy deposited by n and } \gamma \text{ in blanket and reflector}}{\text{Energy of n and } \gamma \text{ incident on blanket}}$

**M_o=Overall energy multiplication = $\dfrac{\text{Energy deposited by n, } \gamma\text{, X, and D in blanket and refl.}}{\text{DT yield}}$

$$M_o = 0.984\,(0.7185 M_n + 0.2815)$$

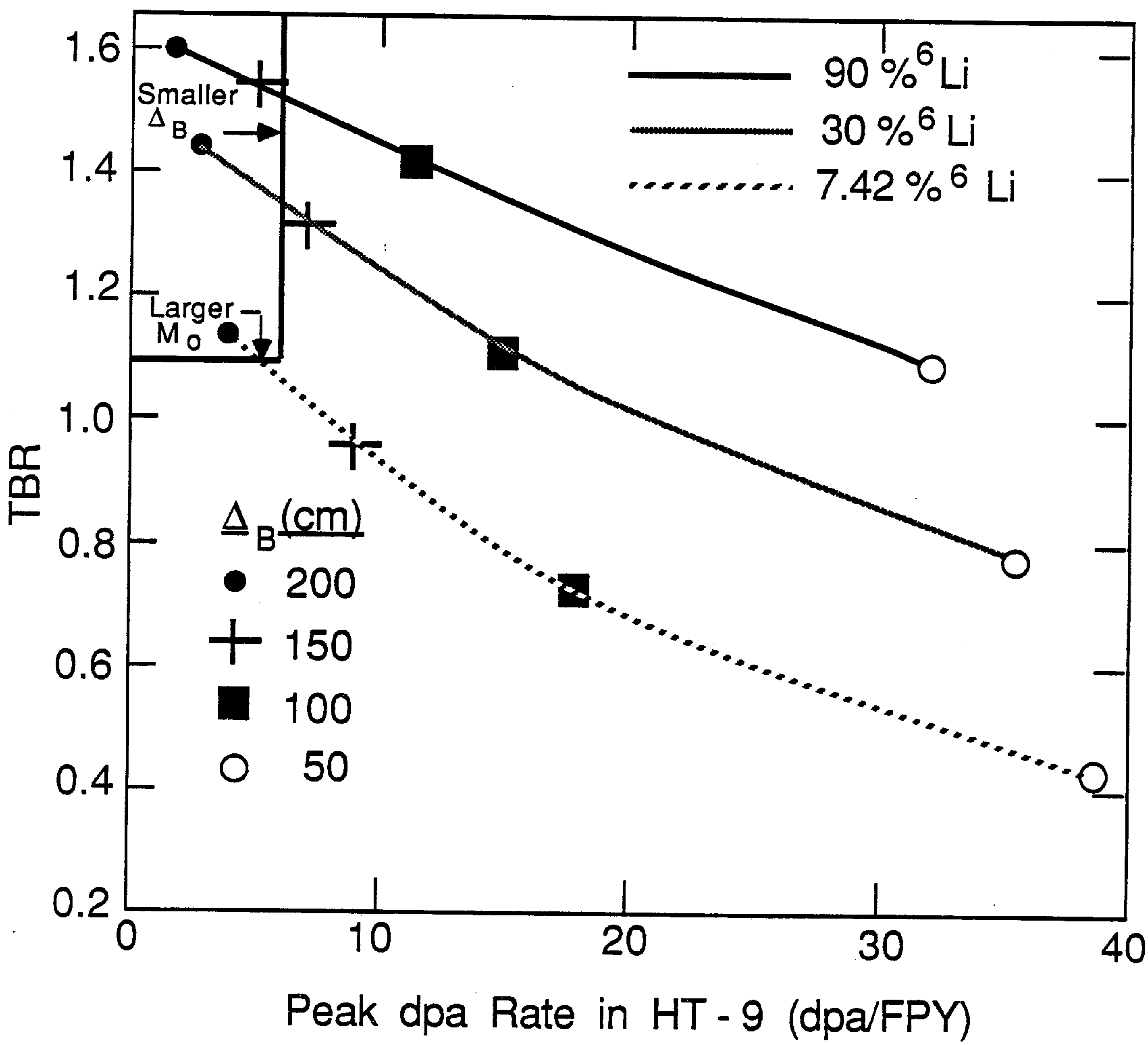

1.6
1.4
1.2
1.0
0.8
0.6
0.4
0.2
TBR
0
10
20
30
40
Peak dpa Rate in HT - 9 (dpa/FPY)
90 %^{6}Li
30 %^{6}Li
7.42 %^{6}Li
Smaller
Δ_B
Larger
M_o
Δ_B(cm)
200
150
100
50

LIBRA Blanket Design Options Satisfying TBR and Damage Requirements (no reflector replacement)

% ^6Li	Δ_B (cm)	TBR	M_o	dpa/FPY	He appm/FPY
90	135	1.5	1.183	6.6	3.5
30	153	1.32	1.215	6.6	2.0
7.42	190	1.1	1.248	4.4	0.8

LIBRA Blanket Design Options Satisfying TBR Requirement with Replaceable Reflector

% ^6Li	Δ_B (cm)	TBR	M_o	dpa/FPY	He appm/FPY	Number of Replacements
90	50	1.1	1.204	31.2	75.2	4
30	100	1.1	1.236	16.07	12.9	2

Conclusions

- If the reflector is designed as a lifetime component, the thinnest blanket can be designed with 90% ^{6}Li leading to a minimum channel length of 4.85 m. The energy multiplication is relatively low and excessive T_2 breeding is obtained.

- If reflector replacement is allowed, using 90% ^{6}Li yields the thinnest blanket with a channel length as small as 4 m being possible. The reflector has to be replaced four times during the reactor life.

- Using natural Li in the LiPb blanket yields the largest energy multiplication but the channel length should be at least 5.4 m.

INPORT Response Code Development

- Planar – linear motion
  Fundamental mode only

- Planar – linear motion
  Fifteen modes

- Planar – linear motion
  Fifteen modes
  Coriolis acceleration (fluid)

- Planar – nonlinear motion
  Fifteen modes
  Coriolis acceleration (fluid)
  Cubic transverse displacement terms

- Nonplanar motion
  Fifteen modes
  Coriolis acceleration (fluid)
  Cubic transverse and lateral displacement terms

VIBRATION AND STABILITY OF VERTICAL TUBES CONVEYING FLUID SUBJECTED TO PLANAR EXCITATION

by

Roxann L. Engelstad

A thesis submitted in partial fulfillment of
the requirements for the degree of

DOCTOR OF PHILOSOPHY
(Engineering Mechanics)

at the

UNIVERSITY OF WISCONSIN–MADISON

1988

INPORT Midspan Displacement History

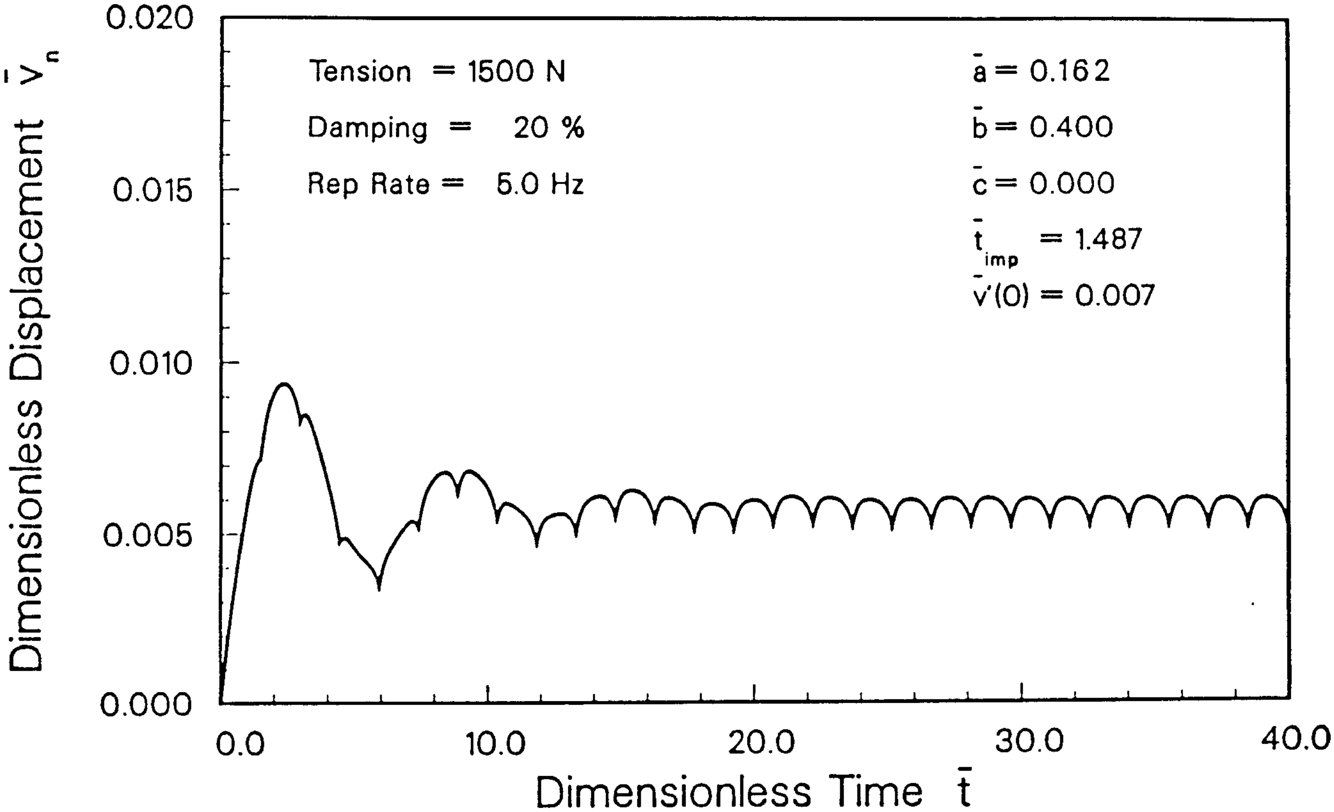

- **Impulse corresponds to 77 Pa-s**
- **Steady state motion develops quickly (~15 shots)**
- **Steady state amplitude is less than 1% of length**

Planar Midspan
Amplitude – Frequency Response

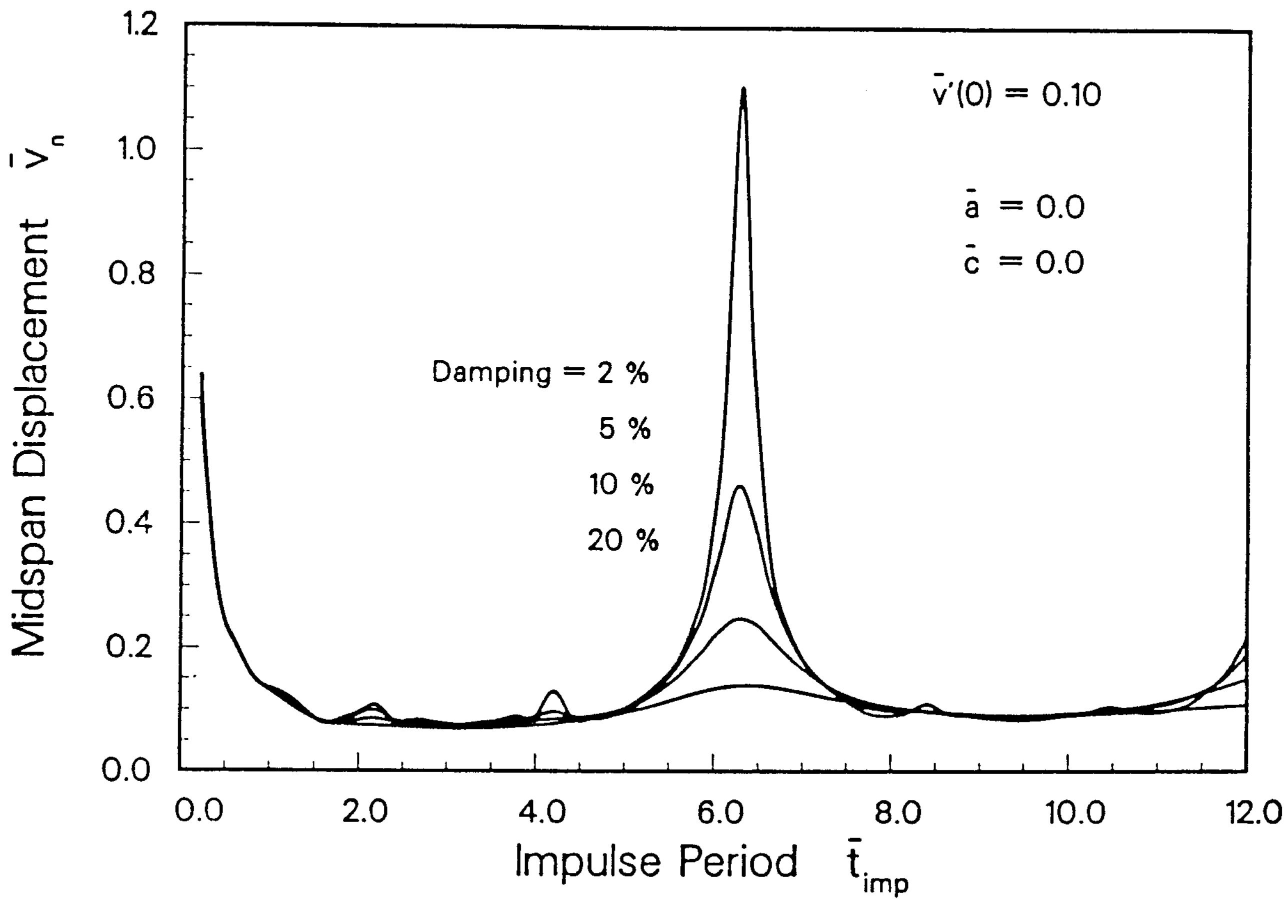

- Figure can be used as parametric design curve with scaling
- Maximum amplitudes occur at resonant rep rates (impulse period)
- Peaks for fundamental mode are highest
- Damping substantially reduces resonant amplitudes

TRITIUM REMOVAL SYSTEMS IN LIQUID BREEDER AND HELIUM COOLANT CIRCUITS

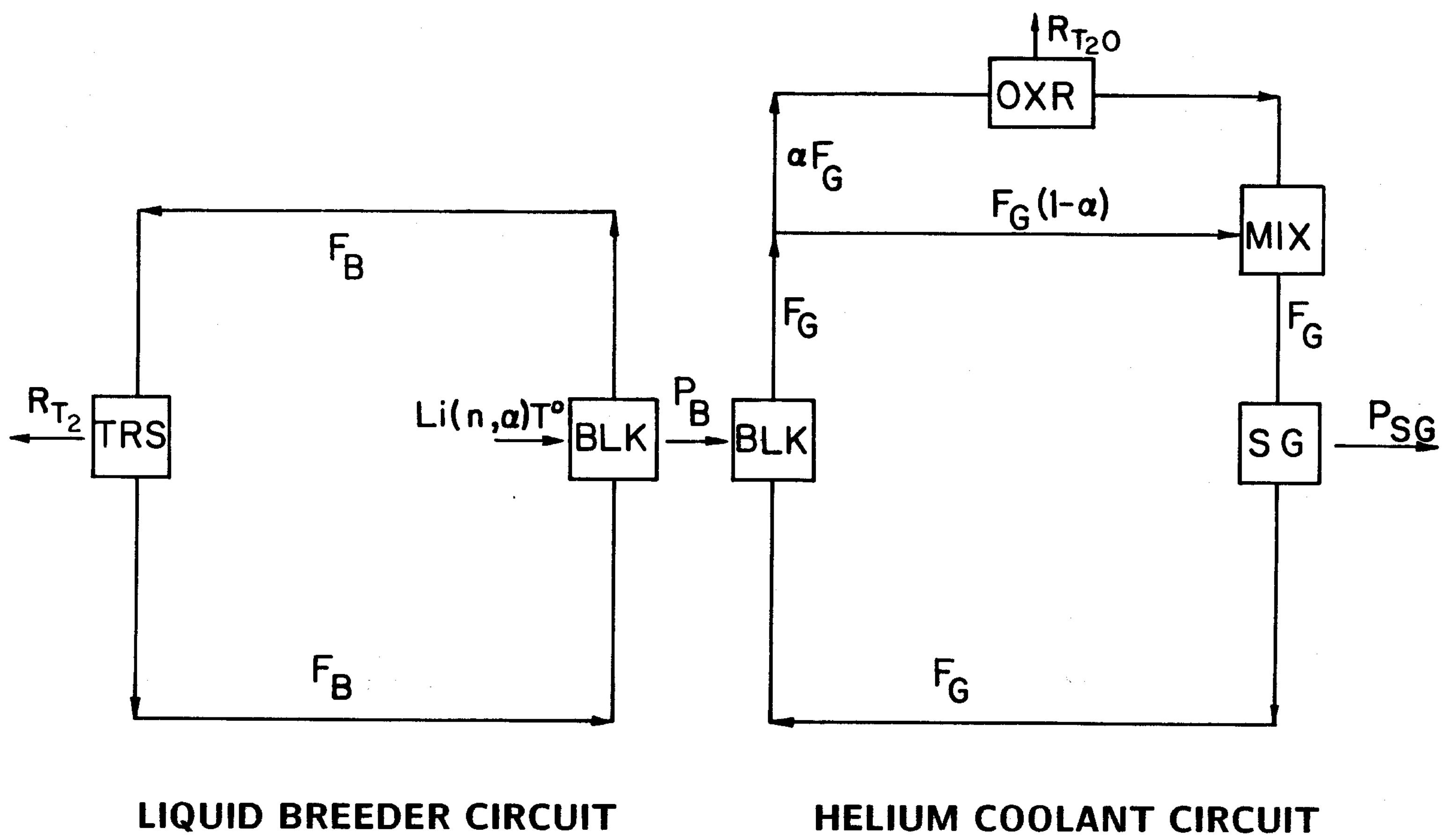

F_B = flow rate of breeder
F_G = flow rate of coolant gas
α = fraction of gas flow to OXR
TRS = Tritium Removal System for liquid breeder
OXR = Tritium Removal by Oxidation & Adsorption

T^o = rate of tritium breeding
P_B = tritium permeation rate to the coolant gas
P_{SG} = tritium permeation rate to the steam circuit
BLK = Breeder liquid to helium coolant heat exchanger
SG = Steam Generator
R_{T_2} = rate of tritium removal

Tritium Inventory

Location	Tritium, g	
In Reactor Hall		
Fuel Supply (1 hr)	21	
Reactor Cavity		
SiC (INPORT tubes)	10	
LiPb (liquid alloy)	0.1	
		31
In Fuel Fabrication Building		
Fuel Processing	20	
Pellet Fabrication	60	
Pellet Storage (1 day)	500	
		580
TOTAL		611